

**INVESTIGATION OF THE POTENCY OF ACYCLOVIR
DERIVATIVES AGAINST HERPES SIMPLEX VIRUS**

CLIVE MOGAKA NYARIBO

MASTER OF SCIENCE

(Molecular Biology and Bioinformatics)

JOMO KENYATTA UNIVERSITY

OF

AGRICULTURE AND TECHNOLOGY

2023

**Investigation of the Potency of Acyclovir Derivatives against Herpes
Simplex Virus**

Clive Mogaka Nyaribo

**A Thesis Submitted in Partial Fulfillment of the Requirements for
the Degree of Master of Science in Molecular Biology and
Bioinformatics of the Jomo Kenyatta University of
Agriculture and Technology**

2023

DECLARATION

This thesis is my original work and has not been presented for a degree in any other University.

Signature: Date:

Clive Mogaka Nyaribo

This thesis has been submitted for examination with our approval as the University Supervisors.

Signature: Date:

Dr. Steven Ger Nyanjom

JKUAT, Kenya.

Signature: Date:

Dr. Florence Atieno Ng'ong'a

JKUAT, Kenya.

DEDICATION

This thesis is dedicated to my late mum, Dinnah Nyaboke who was my first teacher.

ACKNOWLEDGEMENT

I wish to sincerely acknowledge the role played by my university supervisors Dr. Steven Ger Nyanjom and Dr. Florence Atieno Ng'ong'a of the Biochemistry Department, School of Biomedical Sciences, College of Health Sciences for their guidance. I also acknowledge the financial support from a research grant awarded by Africa-ai-Japan Project Innovation Research Grants 2020/2021. I also acknowledge Universal Corporation Limited for providing the Acyclovir API through Dr. Dharmesh. The staffs at the Directorate of Intellectual Property Management and University-Industry Liaison (DIPUIL) were very resourceful as agents for the patent application at the Kenya Industrial Property Institute (KIPI). I also appreciate the staff at Centre for Public Health Research, Kenya Medical Research Institute especially Mr. Samora for the guidance during *in vitro* studies. I extend my gratitude to my wife, Nancy and son, Trevor for the support and time to do research and write this thesis, my brothers Eric, Shem and Wesley and my parents, Mr. Geoffrey Nyaribo and late Mrs. Dinah Nyaribo for their support throughout my studies. Above all I thank Almighty God for the gift of life, knowledge and wisdom.

TABLE OF CONTENTS

DECLARATION	ii
DEDICATION	iii
ACKNOWLEDGEMENT	iv
TABLE OF CONTENTS	v
LIST OF TABLES	viii
LIST OF FIGURES	ix
LIST OF APPENDICES	x
LIST OF ABBREVIATIONS AND ACRONYMS	xi
ABSTRACT	xiii
CHAPTER ONE	1
INTRODUCTION	1
1.1 Background Information	1
1.2 Statement of the Problem	2
1.3 Justification	3
1.4 Research Questions	4
1.5 Null Hypothesis	5
1.6 Objectives	5
1.6.1 General Objective	5
1.6.2 Specific Objectives	5
1.7 Study Limitations	5
CHAPTER TWO	6
LITERATURE REVIEW	6
2.1 Herpes Simplex Virus (HSV).....	6
2.1.1 Epidemiology of HSV	6
2.1.2 Classification of Herpes Viruses	7
2.1.3 Structure of HSV	7
2.1.4 Multiplication and Pathogenesis of HSV	8
2.1.5 Transmission of HSV	9

2.1.6 Clinical Manifestations Associated with HSV	9
2.1.7 Treatment of HSV Infections.....	10
2.2 Computer Aided Drug Design (CADD).....	10
2.3 Molecular Modelling.....	11
2.4 Network Pharmacology	12
2.5 Molecular Docking.....	14
2.6 Quantitative Structure-Activity Relationship.....	14
CHAPTER THREE	16
MATERIALS AND METHODS	16
3.1 Study Design	16
3.2 Molecular Modelling.....	17
3.3 Network Pharmacology	18
3.4 Protein Modelling.....	19
3.5 Molecular Docking.....	19
3.6 Quantitative Structure Activity Relationship (QSAR).....	20
3.7 <i>In vitro</i> Cytotoxicity Studies	20
CHAPTER FOUR.....	23
RESULTS	23
4.1 Molecular Modelling.....	23
4.2 Network Pharmacology.....	26
4.3 Protein Modelling.....	32
4.4 Molecular Docking.....	34
4.5 Quantitative Structure Activity Relationship (QSAR) Analysis.....	36
4.6 Lead Optimization.....	37
4.7 <i>In vitro</i> Studies	38
CHAPTER FIVE.....	40
DISCUSSION	40
5.1 Discussion	40
CHAPTER SIX	42
CONCLUSION AND RECOMMENDATION	42
6.1 Conclusion.....	42
6.2 Recommendations	43

REFERENCES.....	44
APPENDICES.....	60

LIST OF TABLES

Table 2.1: Sub-families of herpes viruses, specific examples and their characteristics.	7
Table 4.1: Molecular descriptors for the 22 derivatives obtained after drugability test based on lipinski's Ro5	23
Table 4.2: IUPAC name for the 22 potential drug compounds.....	25
Table 4.3: Global topological measurements of the HSV PPI network indicating high connectivity	26
Table 4.4: Top 10% node ranking based on centrality measures values with 11 non-repetitive nodes selected for GO.	28
Table 4.5: Top 10% node ranking based on local topological attributes with 13-non repetitive nodes selected for GO.	29
Table 4.6: Functional similarity kappa values of the target nodes with UL5 and US3 having values that meet the threshold.	30
Table 4.7: Binding energies of the acyclovir derivatives when docked against the target proteins with some derivatives having lower binding energies than acyclovir.	34
Table 4.8: Statistical evaluation for drug targets using binding energies.	35

LIST OF FIGURES

Figure 2.1: Estimates of the number of people with HSV-2 infections in 2012 by region.	6
Figure 2.2: The Structure of HSV comprising of the capsid, tegument and envelope.	8
Figure 2.3: FDA approved nucleoside analogues for the treatment of HSV.	10
Figure 2.4: Network showing the associated local topological attributes and centrality measures.	13
Figure 3.1: Resazurin reduction test	21
Figure 4.1: Chemical structures of acyclovir derivatives obtained after drugability test based on Lipinski's Ro5.	24
Figure 4.2: The highly connected HSV PPI Network with majority of the hubs being capsid proteins.	27
Figure 4.3: 3D model representation of (A) DNA replication helicase and, (B) Serine threonine protein kinase.	32
Figure 4.4: The Ramachandran plots for DNA replication helicase indicating a quality model.	33
Figure 4.5: The Ramachandran plots for Serine/threonine protein kinase indicating a quality model.	33
Figure 4.6: Enzyme inhibition scores for acyclovir derivative showing bioactivity scores of the derivatives against thymidine kinase.	36
Figure 4.7: Bioavailability scores for acyclovir derivatives showing absorption and side effects indicators.	37
Figure 4.8: Optimized lead molecule: 2-[(6-methyl-6,9-dihydro-3H-purin- 9yl) methoxy]ethan-1-ol with improved bioavailability.	38
Figure 4.9: Resazurin test showing a seeded well plate before and after addition of resazurin.	38
Figure 4.10: Cytotoxicity study at 24 hours thus lower concentrations required for potency studies.	39
Figure 4.11: Cytotoxicity study at 48 hours, shows that potency studies shall be limited to within 24 hours or less.	39

LIST OF APPENDICES

Appendix I: Research Publication.....	60
Appendix II: Patent Certificate.....	69

LIST OF ABBREVIATIONS AND ACRONYMS

ADMET	Absorption Distribution Metabolism Excretion Toxicity
AIDS	Acquired Immunodeficiency Syndrome
BBB	Blood Brain Barrier
BC	Betweenness Centrality
CADD	Computer Aided Drug Design
CC	Closeness Centrality
DAVID	Database for Annotation, Visualization, and Integrated Discovery
DMEM	Dulbecco's Modified Eagle Medium
DNA	Deoxyribonucleic Acid
EBV	Epstein Barr Virus
EC	Eigenvector Centrality
FBS	Fetal Bovine Serum
FDA	Food and Drug Authority
GO	Gene Ontology
HBA	Hydrogen Bond Acceptors
HBD	Hydrogen Bond Donors
HIA	Human Intestinal Absorption
HIV	Human Immunodeficiency Virus
HSV	Herpes Simplex Virus
IUPAU	International Union of Pure and Applied Chemistry
LAC	Local Average Connectivity

KEMRI	Kenya Medical Research Institute
KIPI	Kenya Industrial Property Institute
MLP	Molecular Lipophilicity potential
NADP	Nicotinamide Adenine Dinucleotide Phosphate
NADH	Nicotinamide Adenine Dinucleotide Hydrogen
MW	Molecular Weight
PDB	Protein Databank
PPI	Protein-Protein Interaction
SMILES	Simplified Molecular-input Line-Entry System
SVM	Support Vector Machine
QSAR	Quantitative Structure Activity Relationship
TCM	Traditional Chinese Medicine
TK	Thymidine Kinase
TPSA	Topological Polar Surface Area
TQ	Thymoquinone
WHO	World Health Organization

ABSTRACT

Herpes simplex virus (HSV) is a prevalent human pathogen with 67% and 13% of the world's population infected with HSV type-1 (HSV-1) and HSV type-2 (HSV-2), respectively. HSV-1 causes oral and perioral infections while, HSV-2 causes genital herpes. Acyclovir, a purine nucleoside analogue, is used for treatment of HSV-1 and HSV-2 infections. The mechanism of action of acyclovir is monophosphorylation by viral thymidine kinase (TK). The emerging HSV resistance to acyclovir due to mutation on viral TK and DNA polymerase necessitates an urgent need for effective strategies to circumvent HSV. This study investigated the potency of acyclovir derivatives against HSV through *in silico* approaches. Ligand-based drug design was used to model acyclovir derivatives on Chemsketch version 2018.2.5. Drugability was determined based on Lipinski's Rule of Five. Putative targets were identified through network pharmacology and validated through gene ontology (GO). Molecular docking was used to determine the binding affinities using Autodock Vina. The pharmacokinetic prediction was done using enzyme inhibition scores on Molinspiration. Pharmacodynamic predictions were based on bioavailability scores on AdmetSAR 2.0. The scores for permeability (Caco2), Blood Brain Barrier (BBB), Human Intestinal Absorption (HIA) and P-glycoprotein inhibitor were generated. The resazurin assay was used to test cytotoxicity. Twenty two acyclovir derivatives had zero violations. 2-[(3, 6-dihydro-9H-purin-9-yl)methoxy]ethan-1-ol had the highest enzyme inhibition score at 1.0 compared to 0.84 for acyclovir. This molecule was optimized to (2-[(6-methyl-6,9-dihydro-3H-purin-9-yl)methoxy]ethan-1-ol, which had a better bioavailability and a higher BBB value of 0.9880 indicating tolerance. DNA replication helicase (UL5) and serine /threonine-protein kinase (US3) were selected based on functional similarity with TK, kappa values were 0.30 and 0.24, respectively. The IC₅₀ of acyclovir at 24 hours and 48 hours were 16.18µg/ml and 38.10µg/ml with R squared values of 0.7894 and 0.9098, respectively. The optimized lead compound, together with its putative targets provides a mechanism to circumvent HSV drug resistance associated with the use of acyclovir. The study recommends *in vitro* and *in vivo* efficacy and toxicity studies for possible development of anti-herpes drug compounds.

CHAPTER ONE

INTRODUCTION

1.1 Background Information

Herpes Simplex Virus (HSV) is a widespread human pathogen. It is estimated that in 2016, approximately 3.7 billion people worldwide were seropositive for HSV type-1 (HSV-1) and nearly 500 million for HSV type-2 (HSV-2) (James et al., 2020). The global prevalence of HSV-1 and HSV-2 is 67% and 13% respectively (Looker et al., 2015) with Africa accounting for 32% of the HSV infections (Looker et al., 2020). Kenyan adults have a higher HSV-2 prevalence rate of 26.6% (Akinyi et al., 2017). In 2007, the Kenya AIDS Indicator Survey (KAIS) provided Kenya's first nationally representative estimate of HSV-2 prevalence rates whereby one third of Kenyans were found to be infected with HSV-2 and 81% of HIV infected persons were coinfecting with HSV-2 (NASCO, 2009).

HSV-1 is highly contagious whereas HSV-2 is a lifelong condition (Zhu et al., 2021). HSV-2 is of particular concern due to its epidemiological synergy with HIV infection and transmission (Knipe et al., 2021). HSV-2 increases susceptibility to HIV infection and immunocompromised persons living with HIV are more likely to be infected with HSV-2. HSV infections are mainly asymptomatic but can cause mild to severe symptoms which include skin blisters and lesions on mucous membranes and genitals, fever during clinical episodes and headache (Crimi et al., 2019).

The WHO recommends, FDA approved drugs namely acyclovir, famciclovir and valaciclovir which are purine nucleosides, for the treatment of HSV infections (WHO, 2016). The mode of action of these drugs involves monophosphorylation by the viral thymidine kinase (TK) (Johnston et al., 2017). Famciclovir and valaciclovir averagely cost USD 6.20 and USD 3.24 per unit of 100 tablets, respectively compared to acyclovir which costs USD 2.19 (Pinder et al., 2014). Side effects such as neurotoxicity and nausea have been reported with the use of valaciclovir (Nunez et al. 2021) and famciclovir (Gopal et al. 2013). Acyclovir is preferred for the treatment

of recurrent clinical episodes of genital HSV infection due to its affordability, tolerability and safety (Alvarez et al., 2020). Acyclovir is converted by viral TK into acyclovir monophosphate which is further converted to acyclovir diphosphate by cellular guanylate kinase and into triphosphate by a number of cellular enzymes. Acyclovir triphosphate competes for the endogenous deoxyguanosine triphosphate (dGTP) and therefore competitively inhibits viral DNA polymerase (Kausar et al., 2021). It is also incorporated into viral DNA, where it acts as a chain terminator because of the lack of 3'-hydroxyl group. The terminated DNA template containing acyclovir binds DNA polymerase and leads to its irreversible inactivation (Jiang et al., 2016).

HSV-1 and HSV-2 elicit lifelong infection and evade the host's immediate antiviral response (Reyes et al., 2021). There is emergence of acyclovir drug resistant HSV especially in immunocompromised patients who require long-term anti-HSV therapy due to recurrent clinical episodes of HSV infections (Zinser et al., 2018). This is caused by mutation on viral TK and DNA polymerase genes (Burrel et al., 2010). Therefore, there is urgent need to identify new targets, design and develop new drug compounds against HSV to circumvent drug resistance.

1.2 Statement of the Problem

HSV infections are among the most common human diseases, and about 80% of the world population is infected by at least one type of HSV which is mostly in latency stage and asymptomatic (Looker et al. 2015). The disease is highly infectious and contagious leading to high number of new infections annually with neonatal infections increasing (WHO, 2016). The cost of treating HSV infections is high with the present value of lifetime direct medical cost estimated to be 972 US Dollars per treated case in 2019. This excludes the costs used to prevent neonatal herpes (Eppink et al., 2021). HSV increases chances of HIV infection hence increasing the transmission rates of the HIV epidemic (Looker et al. 2017). The HSV is associated with the γ -herpes viruses including Epstein–Barr virus (EBV) and Kaposi's sarcoma virus which increase susceptibility to cancer, a leading cause of death (Siegel et al.,

2019). The current drug therapies can only heal sores, prevent new sores from forming and reduce pain but do not fully treat the HSV-2. There is emergence of drug resistant HSV especially in immunocompromised patients who require long-term anti-HSV therapy due to recurrent clinical episodes of HSV infections (Jiang et al., 2016). Severe conditions such as, neurotoxicity especially occur when acyclovir is taken with zidovudine, an HIV regimen drug (Watson *et al*, 2017). The current drug therapies have adverse reactions and side effect such as nausea and vomiting, (Aung et al., 2016); Sharma et al., 2023). Mutagenesis can occur due to the inhibitory effect of acyclovir on cellular DNA polymerase. Acyclovir has low bioavailability thus reduced bioactivity (Hassan et al., 2016).

1.3 Justification

The high infection rates coupled with drug resistance and lack of effective drug therapies to prevent and treat HSV infections necessitates an urgent need for new, effective and efficient strategies and mechanisms to circumvent the viral infections. Genital herpes caused 253000 global disability-adjusted life years (DALYs) in 2019 (https://www.healthdata.org/results/gbd_summaries/2019/genital-herpes-level-4-cause), accounting for 3.4% of DALYs from all sexually transmitted infections. All these severe outcomes disproportionately affect low-income and middle-income countries (Remco et al., 2022).

Computer Aided Drug Design (CADD) has revolutionized the drug development process by drastically reducing the cost and time it takes to discover new and effective drug molecules (Maithri *et al.*, 2016). It is used to expedite and facilitate hit identification, hit-to-lead selection and optimize the absorption, distribution, metabolism, excretion and toxicity profile of drug compounds (Dhingra, 2022). It provides insights that improve precision medicine in lead development and optimization. Further, CADD leverages on recent advancements in artificial intelligence and machine learning in analyzing and explaining pharmaceutical related big data supported by availability of super-computing facility, parallel processing and advance in computer hardware capabilities (Sliwoski, et al., 2014).

CADD has been used to develop therapeutic drug molecules against viral infectious diseases, for instance, Darunavir, a Nonpeptidic HIV-1 protease has been approved for the treatment of HIV/AIDS patients exhibiting multidrug-resistant HIV-1 variants that do not respond to previously existing Highly Active Antiretroviral Therapy (HAART) regimens (Sabe et al., 2021). CADD techniques have been used to develop inhibitors for key viral protein targets of SARS-CoV-2, for instance, homology modeling and Molecular Dynamics (MD) simulation was performed to solve 3D structure of SARS-CoV-2 guanine-N7 methyltransferase (nsp14). The study proposed five Traditional Chinese Medicine (TCM) database compounds (TCM 57025, TCM 3495, TCM 5376, TCM 20111, and TCM 31007) as potential COVID-19 therapeutics (Selvaraj et al., 2020).

Currently the existing research on HSV to address drug resistance has not clearly pointed out alternative putative biological targets for anti-herpetic therapies. There is also, lack of comprehensive drug screening to determine the safety and efficacy of drug molecules. Bhuvad and Samant, 2019, carried out *in silico* drug studies on 13 *Verbascum phlomoides* L. phytochemicals against HSV-1 and HSV-2, however, the study focused on the whole viral structure and did not clearly point out any new putative targets.

Neelabh et. al., 2019 designed a ligand known as NNK that targeted HSV TK and reported acceptable binding affinity. Molecular docking studies on Thymoquinone involving four targets: thymidine kinase, DNA polymerase glycoprotein B, and glycoprotein D concluded that the compound was effective against HSV (Dhanasezhian et al., 2016). However, the study did not indicate its pharmacokinetic or pharmacodynamic properties. Other *in silico* drug repurposing studies on Thiosemicarbazone derivative, against HSV TK indicated good binding energy (Kumar et al., 2021).

1.4 Research Questions

1. What are the acyclovir derivatives modelled and their associated drugability?
2. What are the potential HSV targets?

3. What are the binding affinities (energies) of the acyclovir derivatives when docked against putative HSV targets?
4. What are the pharmacodynamic and pharmacokinetic properties of the acyclovir derivatives?

1.5 Null Hypothesis

The modelled acyclovir derivatives lack inhibitory activity against HSV.

1.6 Objectives

1.6.1 General Objective

To investigate the potency of acyclovir derivatives against HSV through *in silico* approaches.

1.6.2 Specific Objectives

1. To model derivatives of acyclovir and determine their drugability using Lipinski's rule of five.
2. To identify potential HSV targets using network construction techniques and validate them using gene ontology and enrichment analysis.
3. To determine binding affinities of acyclovir derivatives against putative HSV targets by molecular docking.
4. To predict the Quantitative Structure Activity Relationship (QSAR) of the acyclovir derivatives based on pharmacokinetic and pharmacodynamics prediction.

1.7 Study Limitations

Some softwares used for the study require commercial licenses and where student licenses are issued, there is a time limit beyond which one cannot use the software. This was a great challenge during the initial stages of the study.

CHAPTER TWO

LITERATURE REVIEW

2.1 Herpes Simplex Virus (HSV)

The herpes viruses originated from viruses that infected a common ancestor of mammals, birds and reptiles (Virgin, 2014). Evolutionary processes led to selection of variants with altered infectivity and tissue tropism to ensure survival and multiplication (Sehrawat et al., 2018). Herpes viruses have infected many animal species for millions of years. Herpes simplex virus type 1 (HSV-1) has coevolved longest with human ancestors, while herpes simplex virus type 2 (HSV-2) infected humans much later (Wertheim et al., 2014). Both HSV-1 and HSV-2 have the ability to cause local lesions and spread to peripheral neurons, where they remain latent awaiting reactivation (Arvin et al., 2007)

2.1.1 Epidemiology of HSV

Herpes simplex virus infections have very high prevalence rates (WHO, 2020). In 2012, 3.7 billion people (67 %) under the age of 50 had HSV-1 infection while 491 million people (13%) between the age of 15 – 49 had HSV-2 infection (Looker et al., 2015) with sub-Saharan Africa accounting for 32% of the global HSV infections (Looker et al., 2020) as shown in Figure 2.1.

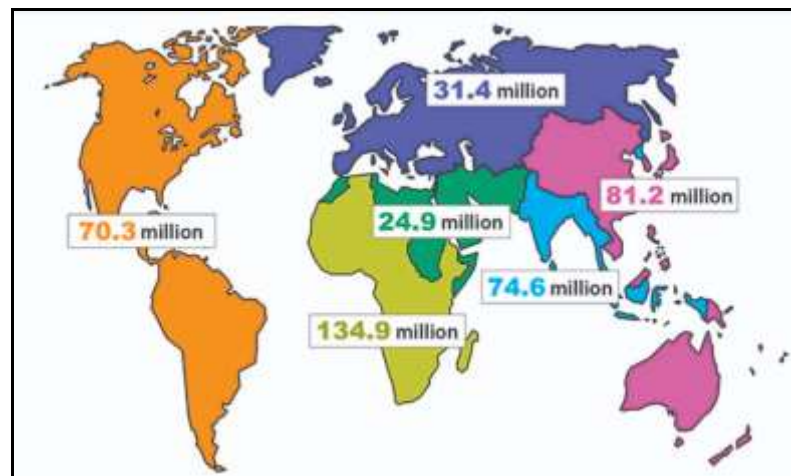


Figure 2.1: Estimates of the number of people with HSV-2 infections in 2012 by region.

2.1.2 Classification of Herpes Viruses

The herpes viruses are broadly classified into three groups, α herpesviruses, β herpesviruses and γ herpesviruses (Whitley, 1996) as shown on Table 2.1.

Table 2.1: Sub-families of herpes viruses, specific examples and their characteristics.

Sub-family	Type of virus	Cycle and host range
α herpesviruses	Varicella-zoster virus (VZV), herpes simplex virus type 1 (HSV-1) herpes simplex virus type 2 (HSV-2)	A short replicative cycle, and a broad host range
β herpesviruses	Cytomegalovirus (CMV), herpesviruses 6 and 7	A long replicative cycle and restricted host range
γ herpesviruses	Epstein-Barr virus (EBV) and human herpesvirus	A very restricted host range

2.1.3 Structure of HSV

HSV is an enveloped, double stranded DNA virus in the *Herpesviridae* family and *Simplex virus* genus (Dai and Zhou, 2018). HSV has a characteristic particle structure comprising of a DNA filled capsid, a proteinaceous tegument layer, and a lipid envelope (Wagner et al., 2008). The capsid protects the genome and functions to release the viral genome into the nucleus of the host cell. HSV glycoprotein D (gD) is essential for virus infectivity and binds to cellular membrane proteins, subsequently promoting fusion between the virus envelope and the cell (Wang et al., 2018). The structure of HSV is illustrated in Figure 2.2.

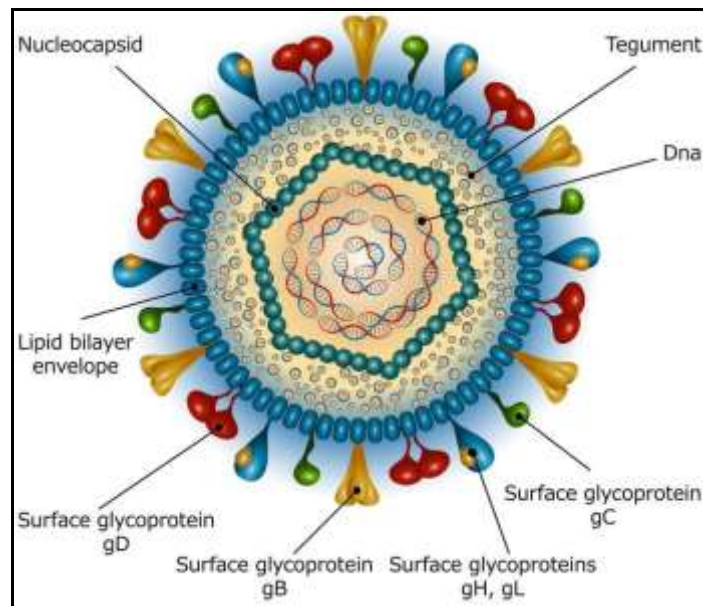


Figure 2.2: The Structure of HSV comprising of the capsid, tegument and envelope.

2.1.4 Multiplication and Pathogenesis of HSV

Transcription, genome replication, and capsid assembly in HSV takes place in the host cell nucleus (Muylaert et al., 2011) Genes are replicated as follows: (i) immediate-early genes, that encode regulatory proteins; (ii) early genes, that encode enzymes for replicating viral DNA; and (iii) late genes, that encode structural proteins (Whitley 1996). The tegument and envelope are acquired as the virion buds out through the nuclear membrane or endoplasmic reticulum. Virions are transported to the cell membrane via the Golgi complex, and the host cell dies as mature virions are released (Rice, 2021)

HSV penetrates susceptible mucosal surfaces or cracked skin (Whitley, 2007). The virus is transported from the epithelial cells to nerve endings and then along peripheral nerve axons through retrograde transport where HSV establishes persistent infection as an episome in the nerve cell bodies in the sacral ganglia and paraspinal ganglia (Cunningham et al., 2006). In the ganglia, HSV enters a state of latency with expression of viral microRNAs and the latency-associated transcript-factors that are crucial for prevention of neuronal apoptosis, maintenance of latency, and regulation

of spontaneous viral reactivation (Schiffer and Corey, 2013). HSV is not cleared from neurons thus, ganglia form lifelong reservoirs of the virus.

Viral replication occurs in the epithelial cells leading to either asymptomatic viral shedding or clinically symptomatic genital ulcer disease (Schiffer et al., 2010). HSV-2 reactivation selectively recruits CD4 cells (HIV target cells) to the genital skin and mucosa thus increased risk for HIV acquisition in HSV-2 seropositive persons (Barnabas and Celum, 2012).

2.1.5 Transmission of HSV

HSV is transmitted through close contact with a person shedding virus at epithelial or mucosal surface, or in genital or oral secretions (Corey and Wald, 2008). HSV-1 is transmitted through oral contact, while HSV-2 is sexually transmitted. HSV can be transmitted perinatally during delivery through direct mucosal or skin contact causing neonatal herpes (James et al., 2014).

2.1.6 Clinical Manifestations Associated with HSV

HSV Primary genital infection is often asymptomatic (Bernstein et al., 2013). Lesions evolve from vesicle pustule to wet ulcers to dry crust (Kimberlin and Rouse, 2004). Multiple genital ulcers, pain, itching, dysuria, vaginal or urethral discharge occurs (Whitley, 2007). Systemic symptoms such as fever, myalgias, headaches, aseptic meningitis also occur. Recurrent symptomatic infection is characterized by a shorter and milder illness (WHO, 2016). Immunocompromised persons, including those with HIV infection, can have severe symptoms and recurrent infections (Strick et al., 2006). Complications related to HSV-2 include meningoencephalitis (brain infection) and disseminated infection. Rarely, HSV-1 infection can lead to more severe complications such as encephalitis (brain infection) or keratitis (eye infection). HSV-2 genital infections increase the risk of acquiring HIV infection. Additionally, persons co-infected with HIV and HSV-2 are more likely to spread HIV to others (Looker et al., 2017). Neonatal herpes occurs in three forms: (i) disease localized to the skin, eye, and mouth (SEM); (ii) encephalitis; and (iii)

neurologic disability or death, thus high child mortality and morbidity (Whitley and Baines, 2018).

2.1.7 Treatment of HSV Infections

Antiviral medications which are nucleoside analogues; acyclovir, famciclovir and valacyclovir are recommended for the treatment of HSV (WHO, 2016). The mode of action for the drugs involves monophosphorylation by the viral thymidine kinase (TK). The chemical structures are shown on Figure 2.3.

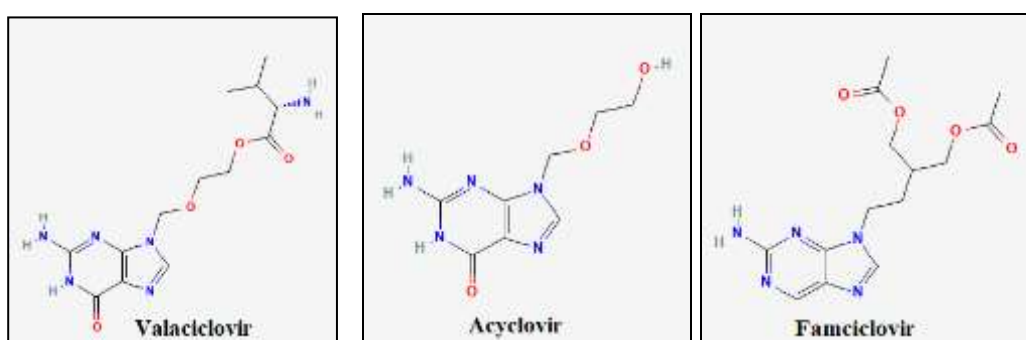


Figure 2.3: FDA approved nucleoside analogues for the treatment of HSV.

The anti-viral drug therapies can help to reduce the severity and frequency of symptoms, but cannot cure the infection (WHO, 2023). HSV antiviral suppressive therapy drastically reduces HSV-2 shedding by 70 to 80%, but it does not eradicate it. Persons with HIV have more severe, prolonged cases of orolabial, genital and perianal infections, suppressive therapy is given in higher doses (Workowski and Bolan, 2015). There is emergence of drug resistance especially in immunocompromised patients, thus, frequent episodes of reactivation, prolonged duration of symptoms and shedding, increased severity of infection, more extensive lesions, atypical lesions, and a greater potential for dissemination, which can even become life-threatening (Birkmann and Zimmermann, 2016).

2.2 Computer Aided Drug Design (CADD)

CADD is an effective method to design and develop drug compounds especially in terms of reducing cost and time spent on drug discovery (Baig *et al.*, 2016).

Conventional drug discovery and development process takes at least ten years, from target identification, high throughput screening, animal model studies to clinical trials for the determination of efficacy and safety of drugs. The process involves trial and error with 90% of the drugs entering clinical trials failing to get FDA approval and reach the consumer market (Leelananda, 2016).

There are two approaches used for CADD: Structure Based Drug Design (SBDD) and Ligand Based Drug Design (LBDD). SBDD approaches including molecular docking, homology modeling, molecular dynamics and structure-based virtual screening have provided insight into ligand-receptor interactions (Wang et al., 2016). LBDD methods such as pharmacophore modeling, Quantitative Structure-Activity Relationship (QSAR) and ligand-based virtual screening provide correlations between chemical features and pharmacological activity. SBDD and LBDD explore drug absorption, distribution, excretion and toxicity (Ferreira, 2018).

2.3 Molecular Modelling

Molecular modelling involves computational techniques for manipulating molecules at the atomistic level and has been applied in drug design, lead identification and optimization (Pimentel et al., 2013). These methods are time saving and cost effective. It has been used to generate new molecular structures based on the structure of known ligands using softwares through building functions such as make bond, break bond, fuse rings, delete atoms and add atoms (Somayeh et al., 2016).

The functional groups are specific moieties of atoms or group of atoms in the structure of molecules that have consistent properties and are responsible for characteristic chemical and biological activity of compounds (Ertl, 2017). At molecular level, functional groups are altered to change the physical and chemical properties of drug compounds or design new drug molecules (Maslehat 2018). The Lipinski rule of five (Ro5) is used to determine drugability. The Ro5 states that a drug molecule shall have no more than five hydrogen bond donors, molecular weight of less than 500 Daltons, not more than ten hydrogen bond acceptors, number of

rotatable bonds should be less than ten and molecular lipophilicity potential should be less than five with polar surface area (PSA) less than 140 Å² (Benet et al., 2016).

2.4 Network Pharmacology

Network pharmacology is based on the principles of network theory and systems biology (Boerries et al.2011). Network pharmacology builds upon systems biology and drug discovery (Boran and Iyengar, 2010). It aims to treat diseases through multiple targets, which can be, either a drug with several targets or a number of drugs with distinct targets (Engin et al., 2014). The approach enhances drug target identification, inferring mechanism of action, drug repurposing, drug synergy, and precision medicine. Network pharmacology aims to understand diseases at the systematic level, the interaction between the drug and the body on the basis of equilibrium theory of biological networks thus providing a paradigm shift regarding the theory and methodology in drug design (Hao and Xiao, 2014). Network pharmacology has been applied in finding drug targets thus enhancing drug efficacy (Zhang, 2016). Network pharmacology increases drug efficacy as it leads to discovery of therapies that are less vulnerable to drug resistance and with few side effects by targeting disease network at the systems level through synergistic interactions (Zhang et al., 2013).

The networks can either be built through *de novo* method which is based on established biological knowledge or *ab initio* which starts from statistical analysis of available data (Xu et al., 2012). There are several softwares for building networks including Cytoscape version 3.0 which accepts data in several standard formats, integrates global datasets and provides powerful visualization tools (Shannon et al., 2003). In analyzing the interactome, the network topological attributes are fundamental. The node is the basic component interacting (pair-wise) with other node(s). This can be a target (enzyme or receptor), gene, disease or drug. The edge is the connection between two nodes which can be physical, regulatory, or genetic. The node degree is the number of links to other nodes. Hubs are nodes with a large number of connections, but there are only a few of them in any network as shown on Figure 2.4, most nodes have few neighbors hence small-scale networks. This is

usually associated with network robustness, the ability of a network to have same behavior even when the various parameters controlling its components change (Chao, 2009).

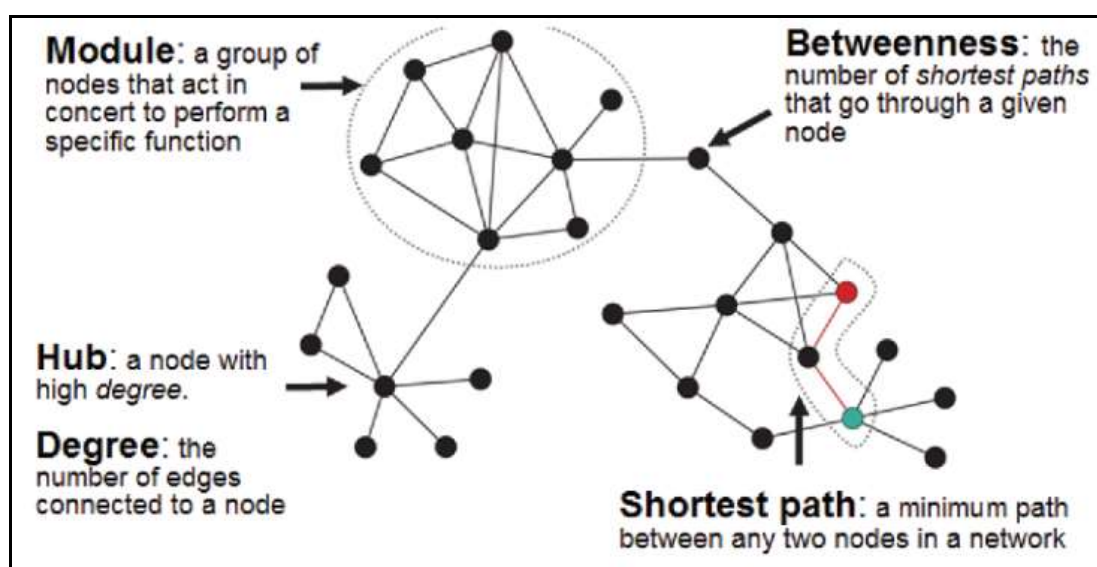


Figure 2.4: Network showing the associated local topological attributes and centrality measures.

Nodes with less connectivity respond poorly to external or internal perturbations. If a drug target is a hub, the consequence may be too much toxicity (Xu et al., 2012). The average separation between arbitrarily chosen nodes is the path length. Centrality is a measure for connectivity within a network (Jesmin et al., 2016). Eccentricity and Closeness centrality (CC) are basically interrelated: CC is the inverse of the average length of the shortest paths. while eccentricity is the maximum distance from the node to all other nodes in a network (Oldham et al., 2019). Degree centrality shows that an important node is involved in a large number of interactions thus transitivity. Closeness centrality indicates important nodes that can communicate quickly with other nodes of the network (Mahyar et al., 2019). Average path length denotes whether nodes are functionally related (Embar et al., 2016). Eigenvector centrality is the measure of the influence of a node while Local Average Connectivity (LAC) is used to identify essential nodes (Li et al., 2011).

2.5 Molecular Docking

Molecular docking predicts the preferred relative orientation of a ligand bound in an active site of the receptor to form a stable complex and it exploits the concept of molecular shape and physicochemical complementarity (Khanna et al., 2019). Molecular docking comprises of two stages: (i) an engine for orientation sampling and (ii) scoring function (Meng et al., 2011). Molecular docking predicts predominant binding mode(s) of a ligand with a protein of known three-dimensional structure. It uses a scoring function to evaluate docking poses by counting the number of favorable intermolecular interactions such as hydrogen bonds and hydrophobic contacts and rank ligands which are most likely to interact favorably to a particular receptor based on the predicted free energy of binding (Morris et al., 2008).

There are three types of molecular docking: rigid, semi-flexible and flexible docking. In rigid docking both the ligand and protein are considered rigid entities with only three translational and three rotational degrees of freedom considered during sampling. (Tripathi and Bankaitis, 2017). This approach is used during protein-protein docking, where the number of conformational degrees of freedom is too high to be sampled. In semi-rigid docking, the ligand is flexible, while the target is rigid (Anderson et al., 2001). Thus, the conformational degrees of freedom of the ligand are sampled, in addition to the six translational plus rotational ones. Flexible docking is based on the concept that a protein is not a passive rigid entity during binding and considers both ligand and protein as flexible counterparts (Andrusier et al., 2008). Different methods have been introduced over the years, some rested on the induced fit binding model while others on conformational selection (Salmaso and Moro, 2018).

2.6 Quantitative Structure-Activity Relationship

Quantitative structure activity relationship (QSAR) models are being built through machine learning approaches based on molecular descriptors of drug compounds (Cherkasov et al., 2014). QSAR uses statistics to establish a quantitative relationship between the structural or physicochemical characteristics and its physiological

activities for a drug compound (Wu and Wang, 2018). Chemoinformatics tools are used to extract, process and extrapolate meaningful data from chemical structures (Lo et al., 2018). Absorption, distribution, metabolism, excretion and toxicity (ADMET) prediction softwares, both web based and command line use machine learning techniques for improved prediction, for instance, ADMET SAR 2.0 uses classification and regression models with highly predictive accuracy (Cheng et al., 2012).

Molecular descriptors are calculated on different levels of representation of molecular structure and then correlated with biological activity using machine learning techniques (Neves et al., 2018). Validated QSAR models are used to predict biological property of novel drug compounds using regression and classification techniques. QSAR modelling has evolved to the modeling and screening of large data sets having diverse chemical structures using a wide range of machine learning techniques (Goh et al., 2017). Data quality problem is a challenge in chemoinformatics, thus, guideline for chemical and biological data curation to allow identification, correction and removal of structural and biological errors in data sets as applicable (Fourches et al., 2016).

Drug have been developed and licensed for viral infections using QSAR models. For instance, oseltamivir a neuraminidase inhibitor as a drug compound was developed against influenza using binary QSAR models applying SVM and Naïve Bayesian methods (Lian et al., 2015). Due to emergence of drug resistance and lack of tolerability, the demand for development of novel anti-HIV is high. Thus, researchers have targeted HIV integrase, an important target involved in viral replication. Using binary QSAR models, 1.5 million of commercially available compounds were screened, 13 molecules were selected for *in vitro* testing with 2 novel chemotypes identified as potential HIV-1 replication inhibitor (Kurczyk et al., 2015).

CHAPTER THREE

MATERIALS AND METHODS

3.1 Study Design

This study involved computer aided drug design techniques, majorly ligand-drug design techniques; molecular modelling and quantitative structure activity relationship (QSAR) and structure-based drug design technique specifically molecular docking. Molecular modelling through Chems sketch was used to design 30 acyclovir derivatives through the alteration of the chemical and physical properties of the acyclovir pharmacophore at the atomic level. This was to increase their bioactivity and bioavailability and, also, circumvent HSV anti-viral therapy drug resistance. Molecular descriptors of the derivatives were determined using Marvin sketch. Virtual screening to determine drugability of modelled derivatives was executed using Lipinski's Rule of Five (Ro5) integrated into a Python code. Network construction, analysis and visualization was carried out using Cytoscape. Ranking of the nodes was done based on centrality measures and local topographical attributes. DAVID database was used for gene ontology (GO) and gene enrichment. GO was used to identify putative biological targets as alternative to TK to circumvent drug resistance caused by mutation on TK and DNA polymerase genes.

Molecular docking was to determine the binding affinities of the acyclovir derivatives against known drug target and identified putative biological targets. The identified putative targets protein structures were modelled since they were unavailable on the Protein Data Bank (PDB). To determine the pharmacokinetics and pharmacodynamics of the acyclovir derivatives, bioavailability was determined using AdmetSAR 2.0 while bioactivity was determined using Molinspiration. Thereafter lead optimization was carried out by the use of molecular modelling techniques. Cytotoxicity studies on acyclovir were carried out using the resazurin test where by vero cells were grown, maintained and seeded in 3 replicates, incubated and proliferation measurements done at two time points; 24 hours and 48hours. *In vitro* data analysis and visualization was done using Graphpad Prism.

3.2 Molecular Modelling

The simplified molecular-input line-entry system (SMILES) format of acyclovir was obtained from Drug Bank (<https://www.drugbank.ca/>) and stored as text file. Chems sketch software version 2018.2.5 was used to model thirty (30) acyclovir derivatives and provide International Union of Pure and Applied Chemistry (IUPAC) nomenclature (ACD, 2019). Ligand based drug design was used to model the acyclovir derivatives to be studied as alternative anti-herpetic drug compounds. The Acyclovir SMILES notation was pasted on Chems sketch and then the molecule manipulated on a two-dimensional space. The acyclovir functional group was manipulated by using Chems sketch functions to design 30 acyclovir derivatives. Open Babel version 2.4.1 was used to convert the acyclovir derivatives to MDL Mol (O'Boyle et al. 2011). The ligands were evaluated for druglikeness.

Drugability or druglikeness defines the physiochemical and structural compound properties of a chemical compound that make it an active drug compound in humans (Bickerton et al., 2012). Drugability or druglikeness of the acyclovir derivatives was evaluated using Lipinski's Rule of Five to select acyclovir derivatives presumed to be biologically active compounds and filter out the non-drug like molecules (Kenakin, 2017). The Lipinski's Rule of five (Ro5) states that drug compound should have Molecular Weight (MW) of less than 500 Daltons and number of Rotatable Bonds (nROTB) should be less than 10. Hydrogen Bond Donors (HBD) and Hydrogen Bond Acceptors (HBA) should be less than 5 and less than or equal to 10 respectively, while the Molecular Lipophilicity Potential (MLP) or xlogP should be less than 5. The Topological Polar Surface Area (TPSA) should be less than 140 Angstrom (Å) (Benet et al., 2016). MarvinSketch, version 19.17, was used to calculate the molecular descriptors of the parent drug, acyclovir and the designed derivatives using the chemoinformatics plugins (ChemAxon, 2019). Python 3 was used to create a sub setting and filtering code in the Jupyter Notebook environment.

3.3 Network Pharmacology

PPI data was downloaded from HVInt 2.0 Database (<http://topf-group.ismb.lon.ac.uk/hvint/>) with the confidence intervals of the interactions ranging from 0.147 to 0.972 including both experimentally supported and computationally predicated interactions (Ashford et al., 2016). The data was mapped from Uniprot accession numbers to open reading frames using HVInt 2.0 Database and validated using Uniprot Mapping/Retrieval Tool (<https://www.uniprot.org/id-mapping>)

Cytoscape 3.0 was used for network construction, visualization and topological analysis (Shannon et al., 2003; Su et al., 2015). Undirected PPI network was created by importing the HSV Proteins interaction data into Cytoscape and assigning the columns appropriately, whereby column A was assigned as the source node, column B as the target node and the confidence scores as the edge attribute. The circular layout was applied. Network editing was done by removing self-nodes, one unconnected node and five single connected nodes. Network analyzer was used to analyze the network's local topological attributes and node size was mapped based on degree and edge size mapped based on confidence score. CytoNCA was used calculate centrality measures of the HSV structural proteins PPI unweighted network; Eigenvector, Local Average Connectivity (LAC), Closeness centrality (CC) and Betweenness centrality (BC) (Oldham et al., 2019). Python 3 was used to rank the nodes to identify a focal node as a presumed biological drug target that can effectively transfer drug effects to its immediate neighbours and affect other more distant neighbours via indirect routes.

The Database for Annotation, Visualization and Integrated Discovery (DAVID, <https://david.ncifcrf.gov/>) was used for GO annotation of the targets selected. The selected nodes were uploaded on the search panel including thymidine kinase (UL23). Using Kappa statistics, the functional similarity between the selected nodes and UL23 was calculated with the Kappa threshold set at $K > 0.20$ (McGee, 2012), the gene list and population background being HSV-1. The semantic similarity of the targets selected to HSV-2 was also calculated since acyclovir can be used for the

treatment of both HSV-1 and HSV-2. Gene enrichment analysis was performed through functional annotation clustering based on Benjamin Correction at $P < 0.05$.

3.4 Protein Modelling

The known acyclovir target, thymidine kinase, was retrieved from PDB (<https://www.rcsb.org/>) and stored in PDB structure format. The 3D protein structures of the helicase primase complex and serine/threonine protein kinase were predicted using trRosetta (Yang et al., 2020) since the proteins were lacking homologs on PDB. *De novo* modelling was used for protein structure prediction. Amino acid sequences were retrieved from Uniprot (<https://www.uniprot.org/>) in fasta format. The sequences were submitted separately to the trRosetta server (<https://yanglab.nankai.edu.cn/trRosetta/>). The trRosetta workflow involve deep residual neural network application to predict the inter-residue distance and orientation distribution which are converted into smooth restraints and the restraints guide Rosetta to build 3D structure models based on energy minimizations (Greener et al., 2019). The models obtained were subjected to evaluation based on the Template Modelling (TM) score which is based on probability of the top predicted distance and the convergence of the top models. TM scores are between 0 and 1, scores below 0.17 correspond to randomly chosen unrelated proteins whereas structures with a score higher than 0.5 assume generally the same fold in SCOP/CATH databases (Xu and Zhang, 2010).

3.5 Molecular Docking

Molecular docking was used to predict the preferred relative orientations of the acyclovir derivatives in the receptor (Target) active sites (Khanna et al., 2019). Protein-ligand docking was used (Ainsley et al, 2018). Autodock Vina Version 1.1.2 which uses united atom scoring function and Broyden-Fletcher-Goldfarb-Shanno (BFGS) algorithm for local optimization was used for molecular docking (Trott and Olson, 2010). Chimera version 1.13.1 which is an integrative graphical tool was used for generating input files for Autodock Vina through ligand, receptor preparation and coordinate setting (Pettersen et al., 2004).

Solvent molecules were deleted from the receptors and further for thymidine kinase the ligand was selected and deleted from the complex. Gasteiger charges and polar hydrogen atoms that are Sybl atom type were added to the receptors. Amber force field parameters were applied. Incomplete side chains were replaced using Dunbrack 2010 rotamer library (Shapovalov and Dunbrack, 2011).

Ligand preparation involved addition of hydrogen atoms and charges using the Add Charge Tool which is a call to Antechamber (Wang et al., 2006). The charge method used was semi-empirical with bond charge correction (AM1BCC). Grid box coordinates for docking were set as follows X centre =31, Y centre = 24 and Z centre = 44. The size points search base were set as X = 22, Y= 24 and Z = 28. During docking number of binding modes were set at 10, search exhaustiveness was set at 8 to attain global minimum.

3.6 Quantitative Structure Activity Relationship (QSAR)

The Molinspiration Bioactivity Predictor (<https://www.molinspiration.com/>) calculated enzyme inhibition scores for 16 acyclovir derivatives including the acyclovir drug by pasting the SMILES files of the molecules to the text window. AdmetSAR 2.0 (<http://lmmd.ecust.edu.cn/admetsar1/>) was used to generate the bioavailability scores for cell permeability (Caco2), blood brain barrier (BBB), human intestinal absorption (HIA) and P- glycoprotein substrate (Yang et al., 2019). Exploratory data analysis and visualization was done Python 3.

3.7 *In vitro* Cytotoxicity Studies

The resazurin assay, also known as Alamar Blue assay was used to test viability of the Vero cells after introduction of acyclovir. Living cells are able to reduce nonfluorescent dye resazurin to the strongly fluorescent dye resorubin.

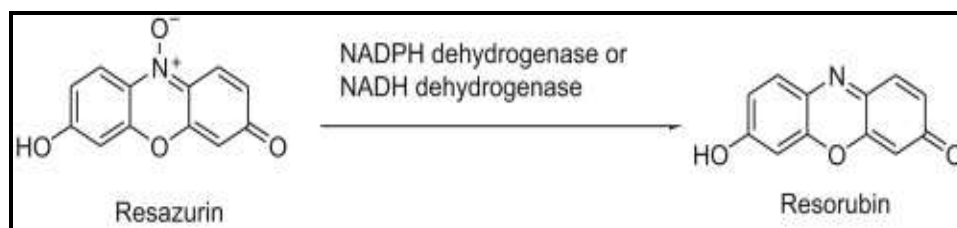


Figure 3.1: Resazurin reduction test.

Vero cells at passage 10 obtained from the Centre for Public Health Research, KEMRI were used for the cytotoxicity studies. Dulbecco's Modified Eagle Medium (DMEM) was used for growth and maintenance. To maintain aseptic conditions, 70% ethanol was used to disinfect surfaces and the cell culture was done in a Biosafety hood.

Growth media contained 1% L-glutamine, 1% Penstrep, 0.1% Gentamycin and 10% Fetal Bovine Serum (FBS). The maintenance media contained was 1% L-glutamine, 1% Penstrep, 0.1% Gentamycin and 2% Fetal Bovine Serum (FBS).

Vero cells being adherent, splitting was done by first washing the cells in a T75 flask with 10ml of Hank's Balanced Salt Solution and adding 1ml of Trypsin. Incubation was done at 37°C and 5% CO₂ for 2 minutes and thereafter the cells were gently agitated. The cells were then split into T25 flasks and 5ml of growth media added and then incubated at 37°C and 5% CO₂.

Microscopy was used to determine that the cells had attained confluent cell monolayers after 3 days of incubation. Cell counting was done by use of a Hauser Scientific Hematocytometer whereby 100µl of cells suspension was mixed with 200µl of Trypanol Blue. The cell density obtained was 2.475×10^5 /ml using the following formulae;

$$\text{Cell density} = \text{Average No. of cells} \times \text{Dilution Factor} \times 10^4$$

The cells were prepared by adding 5.76ml of growth media to 3.84ml of the cell suspension and pipetting repeatedly for proper mixing before dispensing 100ul into each well. Plating/seeding was done on 96 well plates whereby 1×10^4 cells were plated in each well in 3 replicates. Phosphate Buffer Solution (PBS) was used as

solvent to make a stock drug concentration of 100µg/ml. Different drug concentrations were prepared; 6.25µg/ml, 12.5µg/ml, 25.0µg/ml, 50µg/ml and 95µg/ml and PBS as a control by using the stock concentration and growth media by the use of the following formulae;

$$C_1V_1 = C_2V_2$$

After seeding and addition of drug, the 96 well plates were incubated at 37°C and 5% CO₂. The proliferation measurements were done at two time points, 24 hours and 48hours. The wells were then added 30µl of 0.015% resazurin dye, incubated for 4 hours (Markossian et al., 2004) and then cell viability measured using a spectrophotometric well plate reader, Tecan M1000 at 570nm wavelength to assess the effects of acyclovir on vero cells and have documented evidence that the drug does/does not have impact on cell viability. The data obtained was analyzed using Graphpad Prism.

CHAPTER FOUR

RESULTS

4.1 Molecular Modelling

Thirty (30) acyclovir derivatives were modelled and based on Lipinski's Ro5; 22 derivatives (73%) had zero violations as shown by data on Table 4.1.

Table 4.1: Molecular descriptors for the 22 derivatives obtained after drugability test based on Lipinski's Ro5

Derivatives	MW (Da)	nROTB	HBD	HBA	MLP	TPSA(Å)
Acyclovir	225	4	3	7	-1.03	114
1	223	4	3	6	-0.9	97.69
2	224	4	4	7	-1.6	121.54
3	207	3	2	5	0.14	77.46
4	226	4	2	7	-1.31	111.96
6	209	3	2	6	0.01	94.53
7	226	4	3	7	-0.28	108.97
8	297	8	2	8	-0.04	130.06
11	229	4	3	8	-2.66	112.54
12	151	0	3	5	-0.63	96.16
14	226	4	3	6	-1.23	102.4
15	218	2	2	6	-0.07	97.66
16	315	6	3	7	1.46	114.76
17	196	4	2	5	-108	71.67
18	237	5	1	6	-2.44	86.27
19	165	1	1	4	-1.34	67.48
20	195	3	2	5	0.01	77.46
24	309	8	2	7	1.11	120.83
25	266	8	1	5	1.04	60.67
27	225	4	3	7	-0.67	114.76
28	268	8	1	6	-0.39	108.8
29	241	2	2	5	1.65	85.3
30	227	2	2	4	1.24	68.23

The chemical structures of the 22 derivatives with zero violations are shown on Figure 4.1.

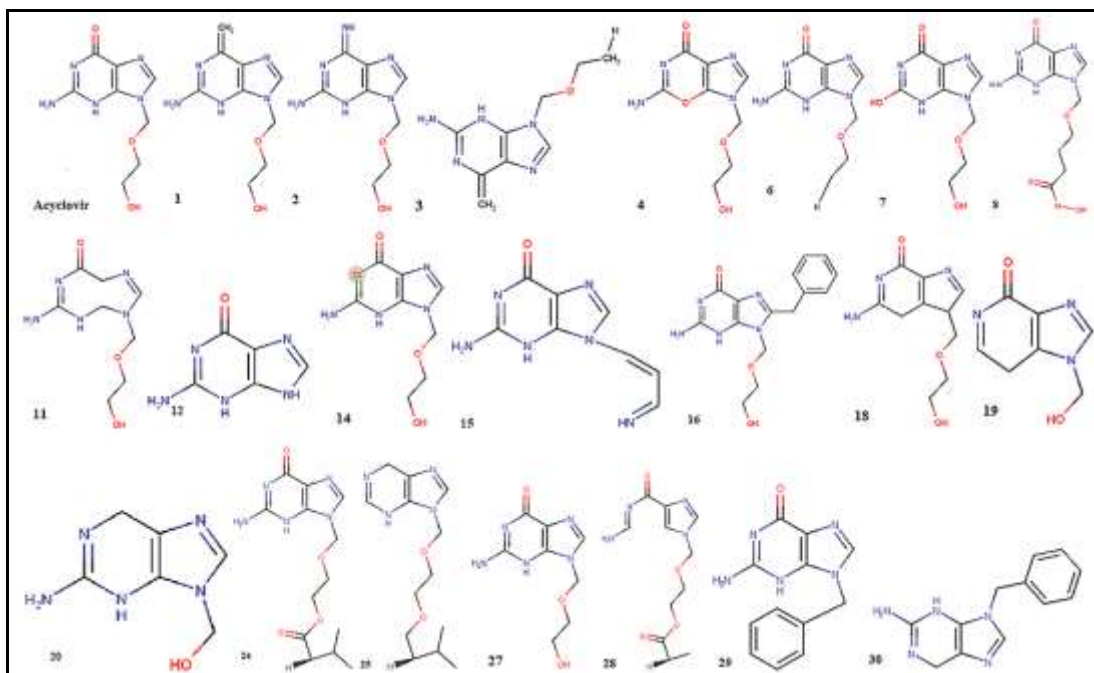


Figure 4.1: Chemical structures of acyclovir derivatives obtained after drugability test based on Lipinski's Ro5.

The modelled acyclovir derivatives have different chemical structures from acyclovir with altered bonds and atoms, thus, anticipated different chemical and biological activity. For instance, ligand number 20 does not have carbonyl group and oxygen atom while ligand number 29 and 30 have additional aromatic ring.

The International Union of Pure and Applied Chemistry (IUPAC) names for the acyclovir derivatives are indicated in Table 4.2.

Table 4.2: IUPAC names for the 22 potential drug compounds

Derivative	IUPAC Name
Acyclovir	2-amino-9-[(2-hydroxyethoxy)methyl]-3,9-dihydro-6H-purin-6-one
1	2-[(2-amino-6-methylidene-3,6-dihydro-9H-purin-9-yl)methoxy]ethan-1-ol
2	2-[(2-amino-6-imino-3,6-dihydro-9H-purin-9-yl)methoxy]ethan-1-ol
3	9-(ethoxymethyl)-6-methylidene-6,9-dihydro-3H-purin-2-amine
4	5-amino-3-[(2-hydroxyethoxy)methyl]imidazo[4,5-e][1,3]oxazin-7(3H)-one
6	2-amino-9-(ethoxymethyl)-3,9-dihydro-6H-purin-6-one
7	2-hydroxy-9-[(2-hydroxyethoxy)methyl]-3,9-dihydro-6H-purin-6-one
8	methyl 4-[(2-amino-6-oxo-3,6-dihydro-9H-purin-9-yl)methoxy]butaneperoxoate
11	(1Z,6Z)-6-amino-3-[(2-hydroxyethoxy)methyl]-3,4,5,9-tetrahydro-8H-1,3,5,7-tetrazonin-8-one
12	2-amino-3,9-dihydro-6H-purin-6-one
14	5-amino-3-[(2-hydroxyethoxy)methyl]-3H,4H,5H,6H,7H-imidazo[4,5-b]pyridin-7-one
15	2-amino-9-[(3Z)-3-(methylimino)prop-1-en-1-yl]-3,9-dihydro-6H-purin-6-one
16	2-amino-8-benzyl-9-[(2-hydroxyethoxy)methyl]-3,9-dihydro-6H-purin-6-one
17	2-[(3,6-dihydro-9H-purin-9-yl)methoxy]ethan-1-ol
18	5-amino-3-[(2-methoxyethoxy)methyl]-3,4-dihydro-7H-pyrrolo[2,3-c]pyridin-7-one
19	1-(hydroxymethyl)-1,7-dihydro-4H-imidazo[4,5-c]pyridin-4-one
20	9-(ethoxymethyl)-6,9-dihydro-3H-purin-2-amine
24	2-[(2-amino-6-oxo-3,6-dihydro-9H-purin-9-yl)methoxy]ethyl 3-methylbutanoate
25	9-[[2-(3-methylbutoxy)ethoxy]methyl]-6,9-dihydro-3H-purine
27	2-amino-9-[(2-hydroxyethoxy)methyl]-3,9-dihydro-6H-purin-6-one
28	2-[(4-[[[(E)-aminomethylidene]carbonyl]-1H-imidazol-1-yl)methoxy]ethyl propanoate
29	2-amino-9-benzyl-3,9-dihydro-6H-purin-6-one
30	9-benzyl-6,9-dihydro-3H-purin-2-amine

4.2 Network Pharmacology

The HSV PPI network shown on Figure 4.2 consisted of 65 nodes and 377 edges hence highly connected. The average degree is 11.6 meaning an individual node is connected to a fairly high number of edges. The mean shortest path length was 2.024 which is fairly low suggesting the nodes are functionally related as shown on Table 4.4

Table 4.3: Global topological measurements of the HSV PPI network indicating high connectivity

Symbol	Description	Value
N	Number of nodes	65
E	Number of edges	377
D	Diameter	4
$\langle k \rangle$	Average degree	11.6
acc	Average clustering coefficient	0.333
mspl	Mean shortest path length	2.024

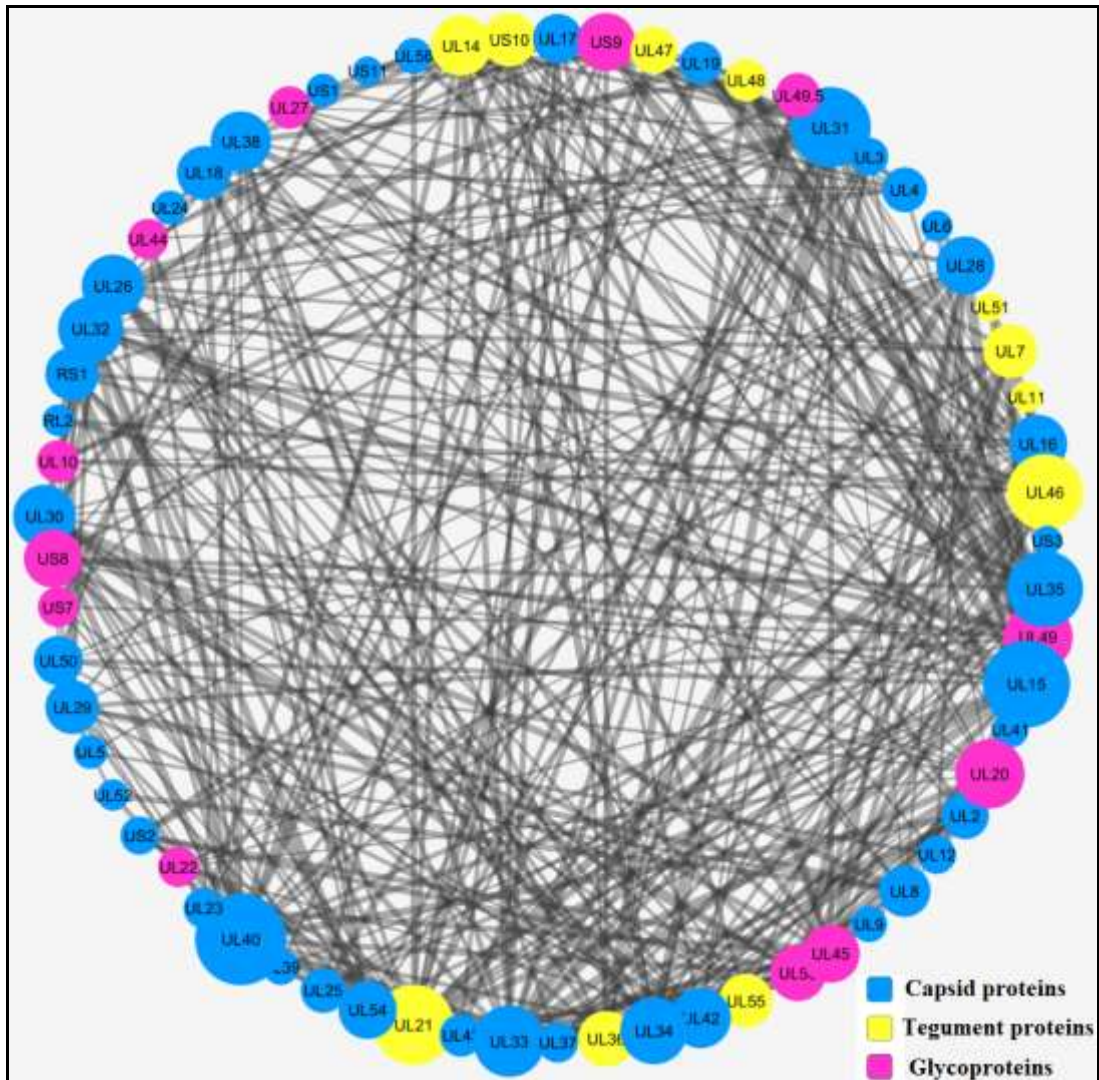


Figure 4.2: The highly connected HSV PPI Network with majority of the hubs being capsid proteins.

Top 10% ranking was done based on local topological attributes (Table 4.4) and centrality measures (Table 4.5). Based on the four centrality measures; - EC, BC, CC and LAC, 11 non-repetitive protein nodes were obtained after ranking: UL40, UL15, UL31, UL21, UL32, UL35, UL34, UL46, UL49, UL33 and UL14.

Table 4.4: Top 10% node ranking based on centrality measures values with 11 non-repetitive nodes selected for GO.

Eigenvector Centrality		Betweenness Centrality		Closeness Centrality		Local Average Connectivity		
Node	Value	Node	Value	Node	Value	Node	Value	
1.	UL40	0.248725	UL40	440.93887	UL40	0.653061	UL32	8.000000
2.	UL15	0.243497	UL15	376.79822	UL15	0.640000	UL31	7.520000
3.	UL31	0.237283	UL21	284.44037	UL31	0.621359	UL34	7.157895
4.	UL21	0.229737	UL35	250.43700	UL21	0.615385	UL15	6.857143
5.	UL32	0.203523	UL46	225.87611	UL34	0.581818	UL21	6.720000
6.	UL35	0.202714	UL49	208.77910	UL46	0.581818	UL40	6.200000
7.	UL34	0.201134	UL31	168.46600	UL33	0.576577	UL14	6.000000

The nodes obtained were the most focal in the network in terms of eccentricity and modularity. Based on neighborhood connectivity, topological and clustering coefficients, radiality, average shortest path length, stress and degree 13 non-repetitive protein nodes were obtained; US3, US11, UL51, UL6, UL11, RL2, UL52, US2, UL5, UL12, UL37, UL3 and UL22.

Table 4.2: Top 10% node ranking based on local topological attributes with 13-non repetitive nodes selected for GO.

S/No.	Neighbourhood Connectivity		Clustering Coefficient		Topological Coefficient		Radiality		Stress		Average Shortest Path Length		Degree	
	Node	Value	Node	Value	Node	Value	Node	Value	Node	Value	Node	Value	Node	Value
1.	US3	23.0	UL11	1.0	US3	0.70	UL40	0.86	UL40	2178	UL40	1.53	UL40	30
2.	UL11	21.0	US2	0.7	US11	0.65	UL15	0.85	UL15	1902	UL15	1.56	UL15	28
3.	UL3	19.8	UL6	0.6	UL51	0.62	UL31	0.84	UL21	1598	UL31	1.60	UL21	25
4.	UL37	19.4	RL2	0.6	UL6	0.53	UL21	0.84	UL35	1418	UL21	1.62	UL31	25
5.	UL6	19.3	UL5	0.6	UL11	0.50	UL46	0.82	UL46	1314	UL46	1.71	UL46	23
6.	UL32	18.8	UL12	0.6	RL2	0.47	UL34	0.82	UL31	1076	UL34	1.71	UL35	23
7.	UL22	18.7	UL37	0.4	UL52	0.42	UL33	0.81	UL49	1026	UL33	1.73	UL33	21

DNA replication helicase (UL5) and serine/threonine protein kinase (US3) were selected as presumed putative biological targets for acyclovir derivatives based on functional similarity with thymidine kinase (UL23) (Table 4.5). ATP binding and nucleotide binding were selected as enriched terms since they are associated with the acyclovir mechanism of action and related genes included UL5 and US3 with significant P value of 0.62 based on Benjamin Correction at $P < 0.05$.

Table 4.3: Functional similarity kappa values of the target nodes with UL5 and US3 having values that meet the threshold.

Target	Name	Cellular Component	Molecular Function	Biological Process	Functional Similarity (UL23)
UL5	DNA replication Helicase	Cell nucleus	ATP binding helicase/Kinase activity	DNA replication	0.30
US3	Serine/threonine -protein kinase	Cell nucleus	ATP binding Kinase activity	Apoptosis	0.24
UL52	DNA primase	Cell nucleus	ATP binding Primase/helicase activity	DNA replication	0.20
RL2	Ubiquitin ligase	Viral envelope	Hydrolase, protease	Gene regulation	0.03
UL3	Nuclear Phosphoprotein	Cell nucleus	Phosphorylation	Colocalization with regulatory proteins	0.00
US2	Unique short glycoprotein	Viral envelope	Mitigation of host immune response	Viral immunoevasion	0.00
UL49	Tegument protein VP22	Viral tegument	RNase activity	Host virus interaction	0.00
UL33	G-protein coupled receptor homolog	Viral envelope	Receptor	Viral immunoevasion	0.00

Target	Name	Cellular Component	Molecular Function	Biological Process	Functional Similarity (UL23)
UL32	Packaging protein	Cell nucleus	Localization of capsids	Packaging Virus genomic DNA	0.00
UL34	Nuclear egress protein	Nuclear membrane	Viral nuclear egress	Viral budding	0.00
UL35	Small Capsomere-interacting protein	Virion	Assembly of virions	Host virus interaction	0.00
UL12	Alkaline nuclease	Viral envelope	DNA binding	Host virus interaction	0.00
UL51	Cytoplasmic envelopment protein	Viral tegument	Cytoplasmic envelopment	Viral budding	0.00
UL37	Inner tegument protein	Viral tegument	Protein binding	Virion assembly	0.00
UL22	Envelope glycoprotein H	Virion membrane	Fusion of viral and plasma membranes	Host virus interaction	0.00
UL11	Cytoplasmic envelopment protein	Viral tegument	Cytoplasmic envelopment	Viral budding	0.00
UL46	Tegument protein	Viral tegument	Activator	Transcription	0.00
UL40	Ribonucleoside-diphosphate reductase	Viral membrane	oxido-reductase	DNA replication Viral latency	0.00
UL31	Nuclear egress protein 1	Viral envelope	Metal ion binding	Viral budding	0.00
UL21	Tegument protein	Viral tegument	Capsid maturation	DNA packaging	0.00
US11	Accessory factor	Cell nucleus	DNA/RNA binding	Host virus interaction	0.00
UL6	Portal protein	Viral envelope	DNA translocation	Viral genome packaging	0.00

Target	Name	Cellular Component	Molecular Function	Biological Process	Functional Similarity (UL23)
UL15	Tripartite terminase subunit	Viral envelope	DNA binding Hydrolase	Viral genome packaging	0.00
UL14	Tegument protein	Viral tegument	Nuclear transport	Viral replication	0.00

4.3 Protein Modelling

The best predicted model for Serine/Threonine Protein kinase (US3) had a TM score of 0.543, while that for DNA replication helicase (UL5) had a TM score of 0.194. Figure 4.3 illustrate the 3D best models for (a) DNA replication helicase and (b) serine/threonine protein kinase (b).

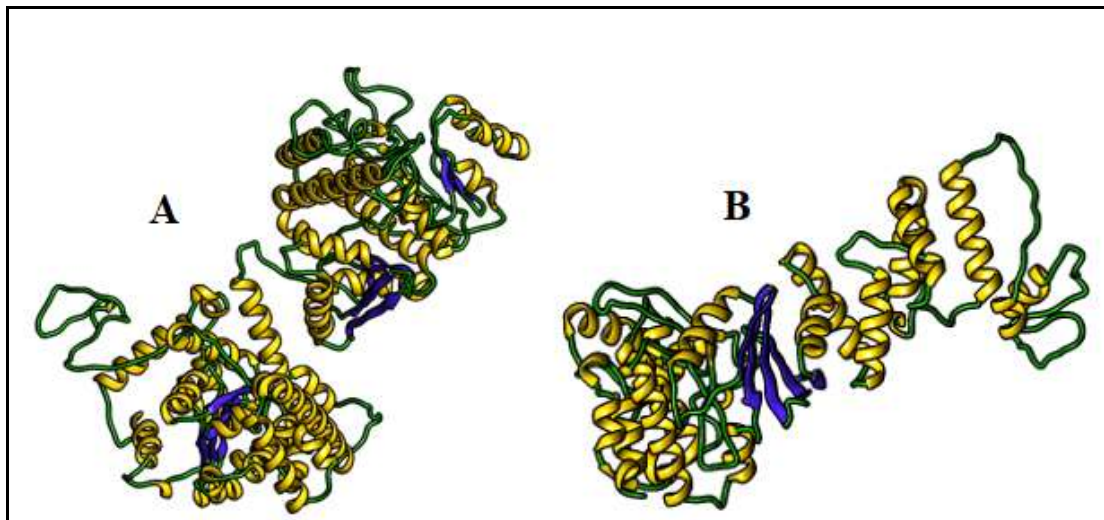


Figure 4.3: 3D model representation of (A) DNA replication helicase and, (B) Serine threonine protein kinase.

The Ramachandran plots for omega, theta and phi torsion angles are illustrated on Figure 4.4 and Figure 4.5 for DNA replication helicase and serine/threonine protein kinase respectively.

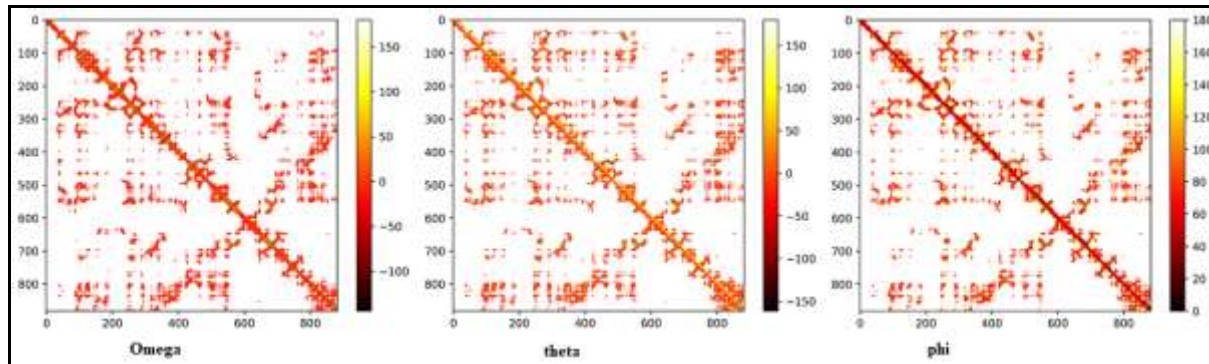


Figure 4.4: The Ramachandran plots for DNA replication helicase indicating a quality model.

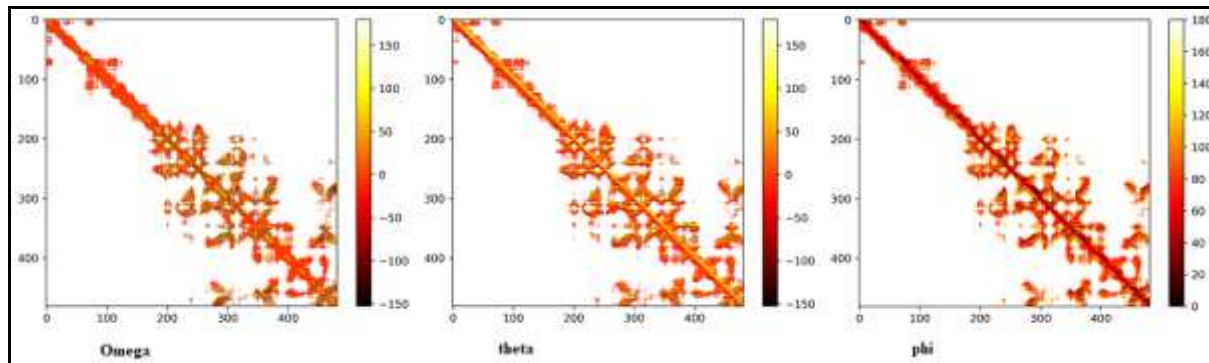


Figure 4.5: The Ramachandran plots for Serine/threonine protein kinase indicating a quality model.

4.4 Molecular Docking

The molecular docking results reported for study are for the best pose between the receptor and the ligand with the Root Mean Square Deviation (RMSD) being 0.00. The lower the binding energies, the orientation is better. 2-amino-9-[(2-hydroxyethoxy)methyl]-3,9-dihydro-6H-purin-6-one (1), 2-[(3,6-dihydro-9H-purin-9-yl)methoxy]ethan-1-ol (17) and 1-(hydroxymethyl)-1,7-dihydro-4H-imidazo[4,5-c]pyridin-4-one (19) had binding energies of -4.7 Kcal/mol while 2-amino-9-[(2-hydroxyethoxy)methyl]-3,9-dihydro-6H-purin-6-one (27) had binding energy of -4.8 Kcal/mol when docked against thymidine kinase. When docked against DNA replication helicase, 2-[(3,6-dihydro-9H-purin-9-yl)methoxy]ethan-1-ol (17) had the lowest binding energy at -6.2Kcal/mol followed by 2-amino-9-[(3Z)-3-(methylimino)prop-1-en-1-yl]-3,9-dihydro-6H-purin-6-one (15) at-6.1Kcal/mol. 2-amino-9-[(2-hydroxyethoxy)methyl]-3,9-dihydro-6H-purin-6-one(1), 9-(ethoxymethyl)-6-methylidene-6,9dihydro-3H-purin-2-amine (3) and 1-(hydroxymethyl)-1,7-dihydro-4H-imidazo[4,5-c]pyridin-4-one (19) had binding energy of 3.6 Kcal/mol, while 2-[(3,6-dihydro-9H-purin-9-yl)methoxy]ethan-1-ol (17) had binding energy of 3.5 Kcal/mol when docked against serine/threonine protein kinase (Table 4.7).

Table 4.4: Binding energies of the acyclovir derivatives when docked against the target proteins with some derivatives having lower binding energies than acyclovir.

Derivative	Thymidine Kinase	DNA replication helicase	Serine Threonine Protein kinase
Acyclovir	-4.6	-6.0	-3.4
1	-4.7	-5.8	-3.6
2	-4.4	-5.9	-3.2
3	-4.6	-5.9	-3.6

Derivative	Thymidine Kinase	DNA replication helicase	Serine Threonine Protein kinase
4	-4.6	-6.0	-3.4
6	-4.6	-5.9	-3.5
7	-4.5	-6.0	-3.4
8	-4.6	-5.9	-3.4
11	-4.5	-5.9	-3.2
12	-4.6	-5.9	-3.4
15	-4.4	-6.1	-3.2
17	-4.7	-6.2	-3.5
18	-4.8	-5.9	-3.4
19	-4.7	-5.7	-3.6
20	-4.5	-5.8	-3.4
27	-4.8	-5.9	-3.2

As per the mean, minimum and maximum binding energies, DNA replication helicase emerged as the best target when compared to the other targets with minimum binding energy of 6.2 Kcal/mol as shown on Table 4.8.

Table 4.5: Statistical evaluation for drug targets using binding energies.

Drug Target	Mean	S. Dev	Minimum	Maximum
Thymidine Kinase	-4.6000	0.1211	-4.8000	-4.4000
DNA replication helicase	-5.188	2.959	-6.200	-5.700
Serine/Threonine Protein Kinase	-3.4000	0.1414	-3.6000	-3.2000

4.5 Quantitative Structure Activity Relationship (QSAR) Analysis

2-[(3,6-dihydro-9H-purin-9-yl)methoxy]ethan-1-ol (17) had the highest enzyme inhibition score at 1.0 compared to 0.84 for acyclovir (Figure 4.6).

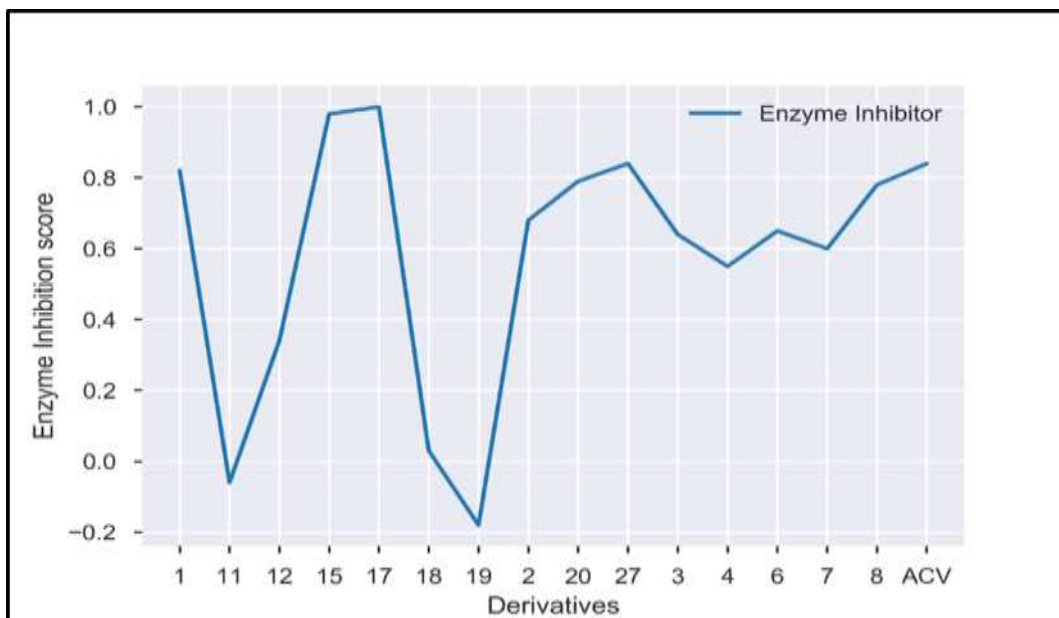


Figure 4.6: Enzyme inhibition scores for acyclovir derivative showing bioactivity scores of the derivatives against thymidine kinase.

The enzyme score for 2-[(3,6-dihydro-9H-purin-9-yl)methoxy]ethan-1-ol is consistent with the lowest binding energies of -6.2Kcal/mol when docked against DNA replication helicase. This molecule lacks oxygen and amino group present in acyclovir. 2-amino-9-[(3Z)-3-(methylimino)prop-1-en-1-yl]-3,9-dihydro-6H-purin-6-one(15) also had an enzyme inhibition score of 0.98 consistent with binding energies of -6.1Kcal/mol. Compared to acyclovir, it lacks an hydrogen and nitrogen atom on the guanine functional group instead of an hydroxide group.

The bioavailability scores for the lead molecules were fairly good, with 2-amino-9-[(3Z)-3-(methylimino)prop-1-en-1-yl]-3,9-dihydro-6H-purin-6-one (15) having a good human intestinal score of 0.9965 which is higher than acyclovir score of 0.9583. 2-[(3,6-dihydro-9H-purin-9-yl)methoxy]ethan-1-ol (17) had a score of 0.9186 as shown on Figure 4.7.

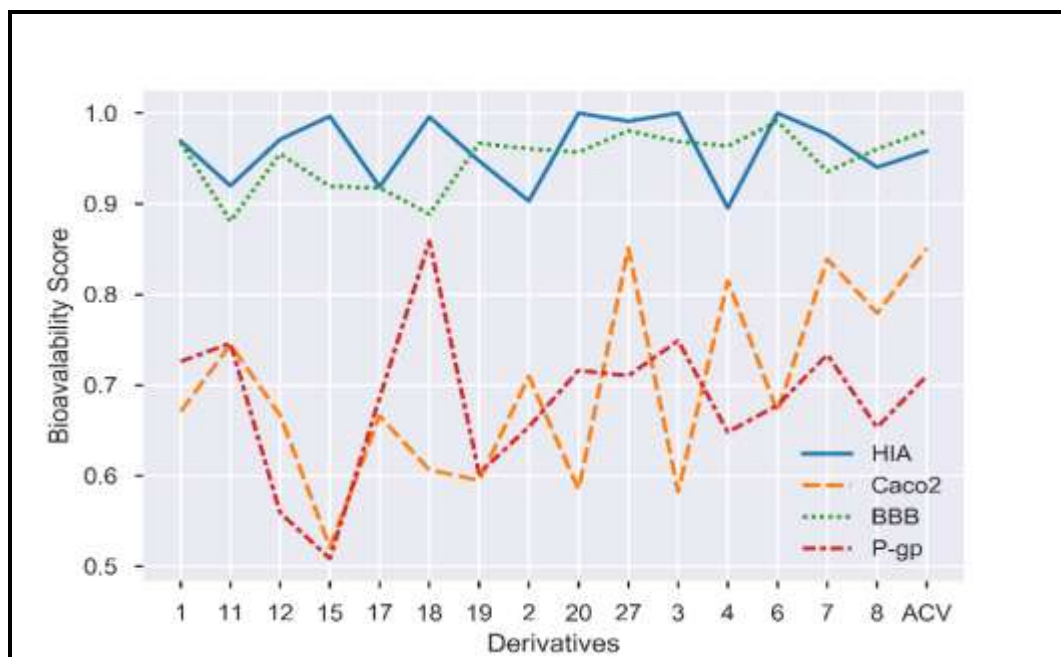


Figure 4.7: Bioavailability scores for acyclovir derivatives showing absorption and side effects indicators.

4.6 Lead Optimization

The lead compounds, 2-[(3,6-dihydro-9H-purin-9-yl)methoxy]ethan-1-ol (17) and 2-amino-9-[(3Z)-3-(methylimino)prop-1-en-1-yl]-3,9-dihydro-6H-purin-6-one (15) were optimized. The optimized lead molecule for 2-[(3,6-dihydro-9H-purin-9-yl)methoxy]ethan-1-ol (17), 2-[(6-methyl-6,9-dihydro-3H-purin-9-yl)methoxy]ethan-1-ol had lower binding energies when docked against TK, DNA replication helicase and serine/threonine protein kinase at -5.6 kcal/mol, -4.7 kcal/mol and -4.1 kcal/mol respectively. For TK and Serine/threonine kinase, the values were higher than the initial molecule.

The optimized lead molecule for 9-[(3Z)-3-(methylimino)prop-1-en-1-yl]-3,9-dihydro-6H-purin-6-one (15), 2-amino-9-hydroxy-6,9-dihydro-3H-purin-6-one when docked against TK, DNA replication helicase and serine/threonine protein kinase had binding energies of -5.1 kcal/mol, -4.5 kcal/mol and -5.1 kcal/mol respectively. For TK and Serine/threonine kinase, the values were higher than the initial molecule.

2-[(6-methyl-6,9-dihydro-3H-purin-9-yl)methoxy]ethan-1-ol had an enzyme inhibition score of 0.90, while 2-amino-9-hydroxy-6,9-dihydro-3H-purin-6-one had

an enzyme inhibition score of 0.44 an indicator of low bioactivity. 2-[(6-methyl-6,9-dihydro-3H-purin-9-yl)methoxy]ethan-1-ol had HIA, Caco₂, BBB and P-glycoprotein values of 0.9702, 0.6362, 0.9880 and 0.9717, respectively while the initial molecule had 0.9186, 0.6660, 0.9174 and 0.6861, respectively. Thus, 2-[(6-methyl-6,9-dihydro-3H-purin-9-yl)methoxy]ethan-1-ol was the best optimized lead molecule (Figure 4.8)

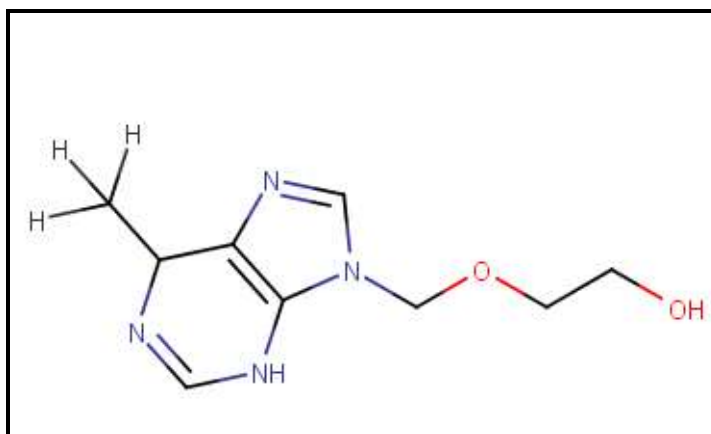


Figure 4.8: Optimized lead molecule: 2-[(6-methyl-6,9-dihydro-3H-purin-9-yl)methoxy]ethan-1-ol with improved bioavailability.

4.7 *In vitro* Studies

The IC₅₀ of acyclovir at 24 hours and 48 hours were 16.18 µg/ml and 38.10 µg/ml with R squared values of 0.7894 and 0.9098 respectively (Figure 4.9 and 4.10). The IC₅₀ values obtained indicate that lower concentrations of the drug shall be applicable for *in vitro* potency and safety pharmacology profiles studies for acyclovir and the synthesized lead molecule.

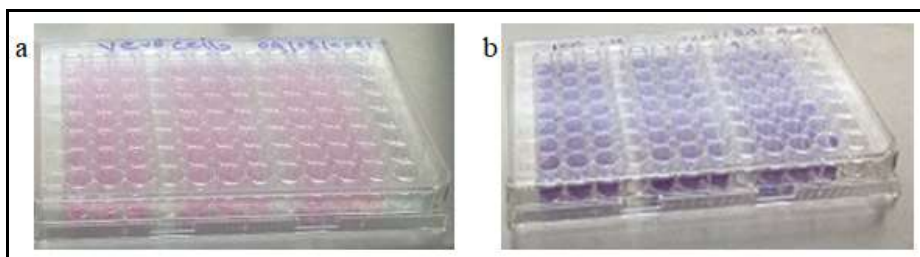


Figure 4.9: Resazurin test showing a seeded well plate before and after addition of resazurin.

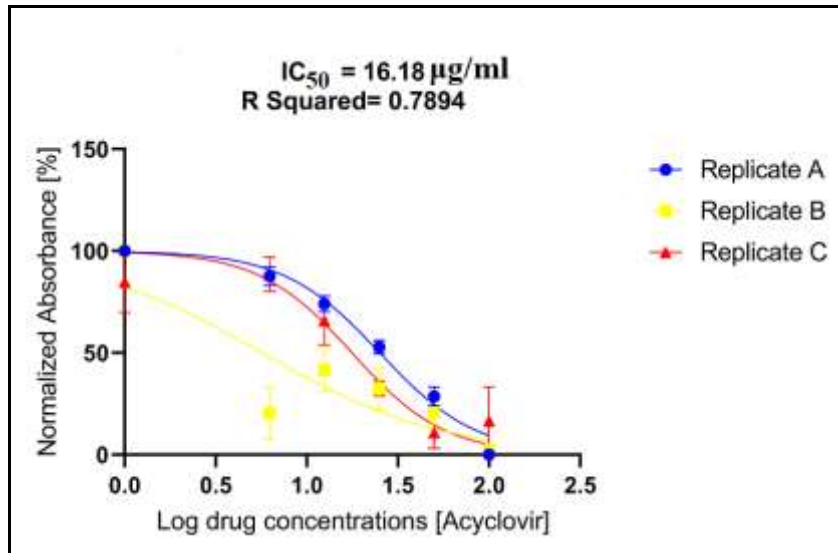


Figure 4.10: Cytotoxicity study at 24 hours thus lower concentrations required for potency studies.

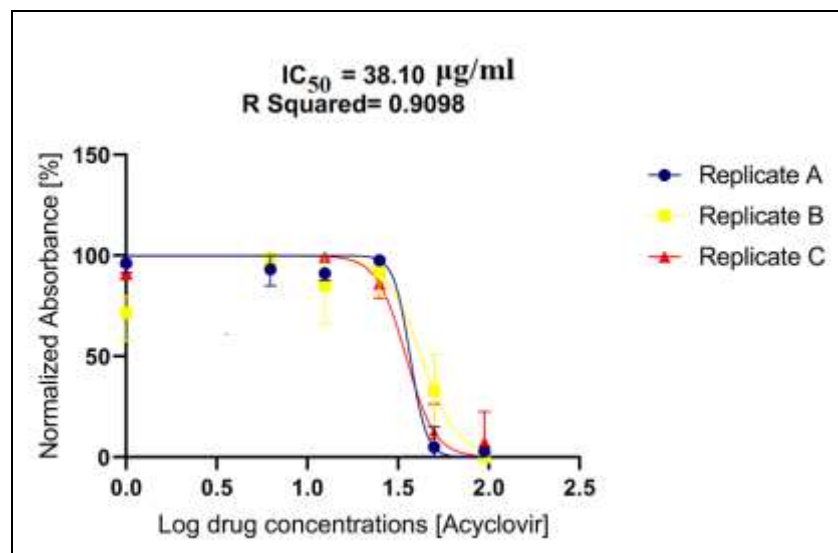


Figure 4.11: Cytotoxicity study at 48 hours, shows that potency studies shall be limited to within 24 hours or less.

CHAPTER FIVE

DISCUSSION

5.1 Discussion

The bioavailability of acyclovir ranges from 10 – 30 % with low permeability (Assis et al., 2021). Out of thirty modelled derivatives, two derivatives 2-[(3,6-dihydro-9H-purin-9-yl)methoxy]ethan-1-ol and 2-amino-9-[(3Z)-3-(methylimino)prop-1-en-1-yl]-3,9-dihydro-6H-purin-6-one emerged as lead compounds with high bioavailability. Although the lead compounds and acyclovir are analogs of the same nucleoside, the slight structure differences between the drugs have led to differences in pharmacology including the human intestinal absorption and cell permeability as was observed for penciclovir (PCV), an anti-HSV guanosine analog with structural differences with acyclovir. PCV had higher affinity for viral TK and viral DNA polymerase as compared to acyclovir thus higher concentrations over prolonged periods in infected cells (Landis, 2021). The 22 acyclovir derivatives modelled also have the potential of being used as alternative HSV drug compounds due to the chemical structure differences with acyclovir, thus addressing the drug resistance associated with acyclovir.

The main mechanism of HSV resistance to nucleoside analogs results from mutations in the thymidine kinase gene (Sadowski et al., 2021). Network pharmacology and gene ontology studies identified putative HSV targets, UL5 and US3 to circumvent HSV drug resistance. The predicted proteins provide potential therapeutic targets for anti-herpes drugs that does not necessarily utilize the thymidine kinase directed pathway. The molecular functions: ATP binding and kinase/helicase activity of the putative targets are as a result of helicase motifs which are involved in viral replication which thus an important aspect in addressing drug resistance (Bermek and Williams, 2021). Anti-herpes drugs target to inhibit viral replication thus control and treat herpes simplex virus infections (Dong et. al., 2021).

Molecular docking results indicated that DNA replication helicase had the lowest mean binding energies followed by serine/threonine protein kinase thus high

bioactivity of the derivatives compared to thymidine kinase as the target. Two derivatives, 2-[(3,6-dihydro-9H-purin-9-yl)methoxy]ethan-1-ol and 2-amino-9-[(3Z)-3-(methylimino)prop-1-en-1-yl]-3,9-dihydro-6H-purin-6-one had lower binding which correlates to the high bioactivity. The compounds with the lowest binding energies compared to their alternatives were selected as lead compounds (Meng et al., 2012). Acyclovir is known to cause adverse effects such as neurotoxicity (Watson et al., 2017), nausea and vomiting (Hassan et al., 2016). Blood brain barrier (BBB) prediction of acyclovir derivatives modelled showed values above 0.90 with the optimized lead having a value of 0.9880 thus reduced side effects to the patient. This shall increase tolerance in patients which shall lead to increased adherence to treatment and overall reduced infection.

The optimized lead compound, 2-[(6-methyl-6,9-dihydro-3H-purin-9-yl) methoxy] ethan-1-ol, has a methyl group and no carbonyl and amine group thus increased bioavailability which is the extent and rate to which the active drug ingredient or active moiety from the drug product is absorbed and becomes available at the site of drug action (Chow, 2014). This modification also, led to increased bioactivity which is the pharmacological action of drug compound, due to increased topological polar surface area. This study developed and optimized a novel acyclovir derivative; 2-[(6-methyl-6,9-dihydro-3H-purin-9-yl) methoxy]ethan-1-ol and evaluated its pharmacodynamics and pharmacokinetics. Similar studies for instance, Neelabh et. al., 2015, designed a ligand known as NNK that targeted the thymidine kinase but, they only evaluated binding affinity through molecular docking. The lead compound is patented with the Kenya Industrial Property Institute (KIPI) under patent number KE 947.

To exclude that inhibitory activities observed during *in vitro* studies are due to cellular alterations caused by acyclovir, cell viability assays were done at different drug concentrations and control. It was found that, the IC₅₀ values of acyclovir at 24 hours and 48 hours were 16.18µg/ml and 38.10µg/ml with R squared values of 0.7894 and 0.9098 respectively. The values indicate potency and shall be used to optimize further *in vitro* assays.

CHAPTER SIX

CONCLUSION AND RECOMMENDATION

6.1 Conclusion

The molecular modelling of acyclovir was successive with 73% of derivatives having zero violations thus passing the Lipinski's Rule of Five (Ro5). The ligand-based drug design technique used for molecular modelling of acyclovir derivatives altered the structure of the pharmacophore of acyclovir and thus its physical, chemical and biological activity thus increased bioavailability and bioactivity.

The identification of putative targets; DNA replication helicase and serine/threonine protein is crucial in circumventing drug resistance associated with the mutation of HSV TK and DNA polymerase genes due to lifelong recurrent clinical episodes caused by HSV infection especially in immunocompromised patients. The biological targets identified could be used to introduce polypharmacology in the design and development of novel synergistic drug therapies against HSV.

Findings from molecular docking showed that 2-[(3,6-dihydro-9H-purin-9-yl)methoxy]ethan-1-ol and 2-amino-9-[(3Z)-3-(methylimino)prop-1-en-1-yl]-3,9-dihydro-6H-purin-6-one had the lowest binding energies when docked against the known target and the identified putative targets compared to the other

Study findings on pharmacokinetic and pharmacodynamic studies involving the designed acyclovir derivative indicate that the acyclovir derivatives have better bioactivity and bioavailability with bioactivity score of 1.0 for ligand 17 and 0.84 for acyclovir.

The lead acyclovir derivative, 2-[(6-methyl-6,9-dihydro-3H-purin-9-yl) methoxy] ethan-1-ol has improved bioavailability and thus can act on the biological target. (2-[(6-methyl-6,9-dihydro-3H-purin-9-yl)methoxy]ethan-1-ol) which is patented with Kenya Industrial Property Institute (KIPI) under Patent Number KE 947 can contribute greatly to the management of HSV infections. The in-silico identification

of the acyclovir derivatives lead compound underscores the importance of computer aided drug design as an alternative method of drug discovery and development.

6.2 Recommendations

The study recommends further *in vitro* and *in vivo* safety and efficacy studies of the 22 derivatives modelled including the lead optimized compound, (2-[(6-methyl-6,9-dihydro-3H-purin-9-yl)methoxy]ethan-1-ol) for possible development of new anti-herpes therapeutic compounds. The study further recommends molecular validation of the two new potential biological targets (DNA replication helicase and serine/threonine protein kinase) as well as other possible new targets for the derivatives.

REFERENCES

- Advanced Chemistry Development, (2019). Chemskech version 2018.2.5, Inc., Toronto, ON, Canada, www.acdlabs.com.
- Ainsley J., Alessio L., Adrian J., Mulholland C., Christov Z., Tatyana G. (2018). Advances in Protein Chemistry and Structural Biology: Combined Quantum Mechanics and Molecular Mechanics Studies of Enzymatic Reaction Mechanisms. *Elsevier*, **111**:1–32. doi: [10.1016/bs.apcsb.2018.07.001](https://doi.org/10.1016/bs.apcsb.2018.07.001)
- Akinyi B., Odhiambo C., Otieno F., Inzaule S., Oswago S., Kerubo E., et al. (2017). Prevalence, incidence and correlates of HSV-2 infection in an HIV incidence adolescent and adult cohort study in western Kenya. *PLoS ONE* **12(6)**: e0178907. <https://doi.org/10.1371/journal.pone.0178907>
- Álvarez M.D., Castillo E., Duarte F.L., Arriagada J., Corrales N., Mónica A. et al. (2020). Current Antivirals and Novel Botanical Molecules Interfering with Herpes Simplex Virus Infection. *Frontiers in Microbiology, Virology*. <https://doi.org/10.3389/fmicb.2020.00139>
- Anderson A.C., O'Neil R.H., Surti T.S. and Stroud R.M (2001). Approaches to solving the rigid receptor problem by identifying a minimal set of flexible residues during ligand docking. *Chemistry and Biology* **.8(5)**:445-57. doi: [10.1016/s1074-5521\(01\)00023-0](https://doi.org/10.1016/s1074-5521(01)00023-0). PMID: 11358692.
- Andrusier N., Mashiach E., Nussinov R., Wolfson H.J. (2008). Principles of flexible protein-protein docking. *Proteins*. **1;73(2)**:271-89. doi: [10.1002/prot.22170](https://doi.org/10.1002/prot.22170). PMID: 18655061; PMCID: PMC2574623
- Arvin A., Campadelli-Fiume G., Mocarski E., Moor S., Roizman B., Whitley R and Yamanishi K. (2007). Human Herpesviruses: Biology, Therapy, and Immunoprophylaxis. Cambridge: *Cambridge University Press*. <https://www.ncbi.nlm.nih.gov/books/NBK47376/>
- Ashford P., Hernandez A., Greco T.M., Buch A., Sodeik B., Cristea I.M., et al. (2016). HVint: A Strategy for Identifying Novel Protein-Protein Interactions in Herpes Simplex Virus Type. *Molecular and Cellular Proteomics*. **15(9)**:2939-2953. doi: [10.1074/mcp.M116.058552](https://doi.org/10.1074/mcp.M116.058552)

- Assis G. S. M., Pedrosa F. C. T., Moraes F. S., Pereira R. G., Souza J. and Ruela M. L. A. (2021). Novel insights to enhance therapeutics with acyclovir in the management of herpes simplex encephalitis, *Journal Pharmaceutical Science* Volume **110** (4):1557–P1671 [doi: 10.1016/j.xphs.2021.01.003](https://doi.org/10.1016/j.xphs.2021.01.003)
- Aung Y. T. and S. Soo (2016) Drugs induced nausea and vomiting; an overview. *Journal of Pharmacy and Biological Sciences*; **11**(3) 5-9. [DOI: 10.9790/3008-1103020509](https://doi.org/10.9790/3008-1103020509)
- Baig M.H, Khurshid A., Mohd A., Zainul A. K., Mohd I. K., Mohtashim L., et al. (2016). Drug Discovery and In Silico Techniques: A Mini-Review. *Enzyme Engineering*; **4**(1) [DOI: 10.4172/2329-6674.1000123](https://doi.org/10.4172/2329-6674.1000123).
- Barnabas R.V. and Celum C. (2012) Infectious co-factors in HIV-1 transmission herpes simplex virus type-2 and HIV-1: new insights and interventions. *Current HIV Research.*; **10**:228-37. [doi: 10.2174/157016212800618156](https://doi.org/10.2174/157016212800618156). PMID: 22384842; PMCID: PMC3563330.
- Bermek O. and Williams R.S. (2021). The three-component helicase/primase complex of herpes simplex virus-1. *Open Biology.* **11**:210011. <https://doi.org/10.1098/rsob.210011>
- Benet L.Z., Hosey C.M., Ursu O. and Oprea T.I. (2016) BDDCS, the Rule of 5 and drugability. *Advanced Drug Delivery Reviews, Elsevier* **1**(101):89-98. [doi: 10.1016/j.addr.2016.05.007](https://doi.org/10.1016/j.addr.2016.05.007). PMID: 27182629; PMCID: PMC4910824.
- Bernstein A. N, Mahesh A., Bandar E.A., Jyoti W., Shree H. and Mueen A. (2013). Enhanced oral bioavailability of acyclovir by inclusion of complex using hydroxypropyl- β -cyclodextrin, *Drug Delivery*. Page 540–547, [doi: 10.3109/10717544.2013.853213](https://doi.org/10.3109/10717544.2013.853213)
- Bernstein D.I., Bellamy A. R., Hook E.W., Levin M.J., Wald A., Ewell M.G., Wolff P.A., Deal C.D., Heineman T.C., Dubin G. and Belshe R.B (2013) Epidemiology, clinical presentation, and antibody response to primary infection with herpes simplex virus type 1 and type 2 in young women.

Clinical Infectious Disease; **56(3):344-51**. [doi:10.1093/cid/cis891](https://doi.org/10.1093/cid/cis891). PMID: 23087395; PMCID: PMC3540038.

Bernstein L. D., Flechtner B. J., McNeil K. L., Heinerman T., Oliphant T. and Tasker S. (2019). Therapeutic HSV-2 vaccine decreases recurrent virus shedding and recurrent genital herpes diseases. *Vaccine*. **37(26)**: 3443-3450. <https://doi.org/10.1016/j.vaccine.2019.05.009>

Bhuvad M.A. and Samant L. R. (2019). In silico docking analysis of phytochemicals from *Verbascum Phlomoides* L. as an antiviral agent against herpes simplex virus Type I and II. *International Journal of Pharmaceutical Science and Research*. Page 1241-1245. [DOI: 10.13040/IJPSR.0975-8232.10\(3\).1241-45](https://doi.org/10.13040/IJPSR.0975-8232.10(3).1241-45)

Bickerton G., Paolini G, Besnard J., Muresan S. and Hopkins L. (2012). Quantifying the chemical beauty of drugs. *Nature Chemistry*. **4(2)**: 90–98. [doi:10.1038/nchem.1243](https://doi.org/10.1038/nchem.1243).

Birkmann A. and Zimmermann H. (2016). HSV antivirals - current and future treatment options. *Current Opinion in Virology*. **18**:9-13. [doi:10.1016/j.coviro.2016.01.013](https://doi.org/10.1016/j.coviro.2016.01.013). PMID: 26897058.

Boerries M., Eils R., Busch H. (2011). Systems Biology. R. A. Meyers, Advances in Molecular Biology and Medicine. Weinheim Germany. *John Wiley and Sons. Inc.* pp 3-32.

Boran A.D., Iyengar R. (2010). Systems approaches to polypharmacology and drug discovery. *Current Opinion Drug Discovery Development*. **13**: 297-309. PMID: 20443163; PMCID: PMC3068535.

Brandariz-Nuñez D., Correas-Sanahuja M. and Maya-Gallego (2021). Neurotoxicity associated with acyclovir and valacyclovir: A systematic review of cases. *Journal of Clinical Pharmacy and Therapeutics*. **46**: 918–926. <https://doi.org/10.1111/jcpt.13464>.

Burrell S., Deback C., Agut H. and Boutolleau D. (2010) Genotypic characterization of UL23 thymidine kinase and UL30 DNA polymerase of clinical isolates of herpes simplex virus: natural polymorphism and mutations associated with

- resistance to antivirals. *Antimicrobial Agents and Chemotherapy*; **54(11)**:4833-42. doi:[10.1128/AAC.00669-10](https://doi.org/10.1128/AAC.00669-10)
- Chao S-Y (2009). Graph Theory and Analysis of Biological Data in Computational Biology, Advanced Technologies. *InTech Open Science*. London. 105-118. DOI: [10.5772/8205](https://doi.org/10.5772/8205)
- ChemAxon (2019). MarvinSketch version 19.17. <http://www.chemaxon.com>.
- Cheng F., Li W., Zhou Y., Shen J., Wu Z., Liu G., et al (2012). AdmetSAR: a comprehensive source and free tool for assessment of chemical ADMET properties. *Journal of Chemical Information and Modeling*; **52(11)**:3099-105. doi: [10.1021/ci300367a](https://doi.org/10.1021/ci300367a) PMID: 23092397.
- Cherkasov A., Muratov E.N., Fourches D., Varnek, A., Baskin, I. I., Cronin, M., et al. (2014) QSAR Modeling: Where have you been? Where are you going to? *Journal of Medicinal Chemistry*; **7**: 4977–5010. doi: [10.1021/jm4004285](https://doi.org/10.1021/jm4004285) PMID: 24351051; PMCID: PMC4074254.
- Corey L. and Wald A. (2008) Genital Herpes. In: Holmes K.K., Sparling P.F., Stamm W.E., et al. (editors). *Sexually Transmitted Diseases*. 4th ed. New York: McGraw-Hill: 399–437.
- Crimi S., Fiorillo L., Bianchi A., D’Amico C., Amoroso G., Gorassini F., et al. (2019). Herpes Virus, Oral Clinical Signs and QoL: Systematic Review of Recent Data. *Viruses*. **11(5)**: 463 doi: [10.3390/v11050463](https://doi.org/10.3390/v11050463)
- Cunningham A.L., Diefenbach R.J., Miranda-Saksena M., Besnjak L., Kim M., Jones C et al. (2006). The cycle of human herpes simplex virus infection: virus transport and immune control. *Journal of Infectious Diseases*; **194**: 11-18. doi: [10.1086/505359](https://doi.org/10.1086/505359) PMID: 16921466.
- Dai X. and Zhou H. Z. (2018). Structure of the Herpes Simplex Virus 1 capsid with associated tegument protein complexes. *Science*. **6**; 360. doi: [10.1126/science.aao7298](https://doi.org/10.1126/science.aao7298)
- Dhanasezhian A., Sasikala S., Singh K.S., Prabhu V., Govindaraju K. and Srivani S. (2016). *In vitro* and *in silico* Evaluation of Anti-herpes simplex virus

Potentials of Thymoquinone. *2nd International Conference on Structural and Functional Genomics*. School of Chemical and Biotechnology, SASTRA University.

Dhingra, N. (2022). Computer-Aided Drug Design and Development: An Integrated Approach. *Drug Development Life Cycle*. doi: [10.5772/intechopen.105003](https://doi.org/10.5772/intechopen.105003)

Dong H, Wang Z, Zhao D, Leng X, Zhao Y (2021). Antiviral strategies targeting herpesviruses. *Journal of Virus Eradication*. **30;7(3):100047**.doi: [10.1016/j.jve.2021.100047](https://doi.org/10.1016/j.jve.2021.100047). PMID: 34141443;

Embar V., Handen A., Ganapathiraju M. K. (2016). Is the average shortest path length of gene set a reflection of their biological relatedness? *Journal of Bioinformatics and Computational Biology*. doi: [10.1142/S0219720016600027](https://doi.org/10.1142/S0219720016600027). PMID: 28073302; PMCID: PMC5726383

Engin B.H, Gursoy A., Nussinov R. and Keskin O. (2014). Network-Based Strategies Can Help Mono- and Poly-pharmacology Drug Discovery: A Systems Biology View. *Current Pharmaceutical Design*; **20(8):1201-1207**. doi: [10.2174/13816128113199990066](https://doi.org/10.2174/13816128113199990066) PMID: 23713773.

Eppink S.T., Kumar S., Miele K., Chesson H.W. (2021). Lifetime Medical Costs of Genital Herpes in the United States: Estimates from Insurance Claims. *Sex Transmitted Diseases*. **48(4):266-272**. doi: [10.1097/OLQ.0000000000001371](https://doi.org/10.1097/OLQ.0000000000001371)

Ertl, P. (2017). An algorithm to identify functional groups in organic molecules. *Journal of Cheminformatics* **9;36** <https://doi.org/10.1186/s13321-017-0225-z>

Ferreira L.L.G., Andricopulo A.D. (2018). Chemoinformatics Approaches to Structure- and Ligand-Based Drug Design. *Frontiers in Pharmacology*. **4(9):1416**. doi: [10.3389/fphar.2018.01416](https://doi.org/10.3389/fphar.2018.01416).

Fourches D., Muratov E. and Tropsha A. (2016). Trust but verify II: A practical guide to chemogenomics data curation. *Journal of Chemical Informatics* **56: 1243-1252**. DOI: [10.1021/acs.jcim.6b00129](https://doi.org/10.1021/acs.jcim.6b00129).

- Goh G.B., Hodas N.O. and Vishnu A. (2017). Deep learning for computational chemistry. *Journal of Computational Chemistry*. **38**: 1291-1307. <https://doi.org/10.1002/jcc.24764>
- Gopal M. G., Shannoma, Kumar B C S, Ramesh M., Nadini A. S. and Manjunath N.C. (2013). A comparative study to evaluate the efficacy and safety of acyclovir and famciclovir in the management of herpes zoster. *Journal of Clinical and Diagnostic Research*;7(12):2904-7. [doi: 10.7860/JCDR/2013/7884.3670](https://doi.org/10.7860/JCDR/2013/7884.3670) PMID: 24551671; PMCID: PMC3919380.
- Greener, J.G., Kandathil, S.M. & Jones, D.T. (2019). Deep learning extends de novo protein modelling coverage of genomes using iteratively predicted structural constraints. *Nature Communications* **10**, 3977. <https://doi.org/10.1038/s41467-019-11994-0>
- Hao C. D and Xiao G. P. (2014). Network Pharmacology: A Rosetta Stone for Traditional Chinese Medicine. *Drug Development Research*. **75 (5)**: 299-312. <https://doi.org/10.1002/ddr.21214>
- Hassan H., Khadija A., Fauziah A., Shamsuddin F. and Basir R. (2016). Antiviral nanodelivery systems: Current trends in acyclovir administration. *Hindawi*. Article ID 4591634. <https://doi.org/10.1155/2016/4591634>
- James S.H., Sheffield J.S., Kimberlin D.W. (2014). Mother-to-Child Transmission of Herpes Simplex Virus. *Journal of Pediatric Infectious Disease Society*. [doi: 10.1093/jpids/piu050](https://doi.org/10.1093/jpids/piu050). PMID: 25232472; PMCID: PMC4164179.
- James C., Harfouche M., Welton N.J., Turner K.M., Abu-Raddad L.J., Gottlieb S.L., Looker K.J. (2020). Herpes simplex virus: global infection prevalence and incidence estimates, 2016. *Bull World Health Organization*. 1;98(5):315-329. [doi: 10.2471/BLT.19.237149](https://doi.org/10.2471/BLT.19.237149). Epub 2020 Mar 25. PMID: 32514197; PMCID: PMC7265941.
- Jesmin T., Waheed S, Emran A.A. (2016). Investigation of common disease regulatory network for metabolic disorders: A bioinformatics approach. *Network Biology*; **6(1)**: 28-36.

- Jiang C-Y., Feng H., Lin C-Y and Guo R-X (2016). New strategies against drug resistance to herpes simplex virus. *International Journal of Oral Science*; 8(1): 1–6. DOI: [10.1038/ijos.2016.3](https://doi.org/10.1038/ijos.2016.3)
- Johnston C. and Wald A. (2017). *Infectious Diseases, Genital Herpes; Antiviral therapy*. Elsevier. Fourth Edition. <https://doi.org/10.1016/C2013-1-00044-3>
- Kausar S., Said Khan F., Ishaq Mujeeb Ur Rehman M., Akram M., Riaz M., Rasool G., Hamid Khan A., Saleem I., Shamim S. and Malik A. (2021) A review: Mechanism of action of antiviral drugs. *International Journal of Immunopathology and Pharmacology*. doi: [10.1177/20587384211002621](https://doi.org/10.1177/20587384211002621)
- Kenakin P. T., (2017) *Pharmacology in drug discovery and development: Understanding Drug Response*, 2nd Edition. Elsevier <https://doi.org/10.1016/C2015-0-00443-9>
- Khanna V., Ranganathan S. and Petrovsky N. (2019) Encyclopedia of Bioinformatics and Computational Biology: Rational Structure-Based Drug Design. *Elsevier* 2:585-600. <https://doi.org/10.1016/B978-0-12-809633-8.20275-6>
- Kimberlin D.W., Rouse D.J. (2004). Clinical practice. Genital herpes. *New England Journal Medicine*. 6;350(19):1970-7. doi: [10.1056/NEJMc023065](https://doi.org/10.1056/NEJMc023065). PMID: 15128897.
- Knipe M. D. and Whitley R. (2021). *Encyclopedia of Virology: Herpes Simplex Virus 1 and 2*. Fourth Edition. *Academic Press*. <https://doi.org/10.1016/B978-0-12-809633-8.21273-9>
- Krishnan R and Stuart M. P. (2021). Developments in vaccination for herpes simplex virus. *Frontiers in Microbiology*. <https://doi.org/10.3389/fmicb.2021.798927>
- Kurczyk A., Warszycki D., Musiol R., Kafel R., Bojarski A.J., Polanski J. (2015) Ligand-Based Virtual Screening in a Search for Novel Anti-HIV-1 Chemotypes. *Journal of Chemical Information and Modelling*. 26;55(10):2168-77. doi: [10.1021/acs.jcim.5b00295](https://doi.org/10.1021/acs.jcim.5b00295)

- Landis M. N. (2021). Topical and Intralesional Antiviral agents: A comprehensive Dermatologic Drug Therapy, 4th Edition, *Elsevier*. pp. 493–503. ISBN 9780323612111, doi: [10.1016/B978-0-323-61211-1.00043-7](https://doi.org/10.1016/B978-0-323-61211-1.00043-7)
- Leelananda S. P., and Lindert S. (2016) Computational methods in drug discovery. *Beilstein. Journal of organic chemistry*; 12:2694-2718. <https://doi.org/10.3762/bjoc.12.267>
- Li M., Wang J., Chen X., Wang H. and Pan Y. (2011) A local average connectivity-based method for identifying essential proteins from the network level. *Computational Biology and Chemistry*.;35(3):143-50. doi: [10.1016/j.compbiolchem.2011.04.002](https://doi.org/10.1016/j.compbiolchem.2011.04.002) PMID: 21704260.
- Lian W., Fang J., Li C., Pang X., Liu A.L., Du G.H. (2016). Discovery of Influenza A virus neuraminidase inhibitors using support vector machine and Naïve Bayesian models. *Molecular Diversity*. 20(2):439-451. doi: [10.1007/s11030-015-9641-z](https://doi.org/10.1007/s11030-015-9641-z)
- Lo C-Y, Rensi E. S., Torng W. and Altman B. R. (2018). Machine learning in chemoinformatics and drug discovery. *Drug Discovery Today*;23: 1538-1546. doi: [10.1016/j.drudis.2018.05.010](https://doi.org/10.1016/j.drudis.2018.05.010) PMID: 29750902; PMCID: PMC6078794.
- Looker K. J., Magaret A. S., May M. T., Turner K. M., Vickerman P., and Gottlieb S. L., (2015). Global and Regional Estimates of Prevalent and Incident Herpes Simplex Virus Type 1 Infections in 2012. *PLoS ONE*;10(10): 1371. <https://doi.org/10.1371/journal.pone.0140765>
- Looker K.J., Elmes J.A.R., Gottlieb S.L., Schiffer J.T., Vickerman P., Turner K.M.E., Boily M.C. (2017). Effect of HSV-2 infection on subsequent HIV acquisition: an updated systematic review and meta-analysis. *Lancet Infectious Diseases*; 17(12):1303-1316. doi: [10.1016/S1473-3099\(17\)30405-X](https://doi.org/10.1016/S1473-3099(17)30405-X) PMID: 28843576; PMCID: PMC5700807
- Looker K. J., Welton N. J., Sabin K. M., Dalal S., Vickerman P., Turner K. M. E., et al. (2020). Global and regional estimates of the contribution of herpes simplex virus type 2 infection to HIV incidence: a population attributable

- fraction analysis using published epidemiological data. *Lancet Infectious Disease*. doi: 10.1016/S1473-3099(19)30470-0.
- McGee S. (2012) Evidence-Based Physical Diagnosis: Reliability of physical findings. 3rd Edition. Pages 29-39. <https://doi.org/10.1016/B978-1-4377-2207-9.00004-5>
- Mahant A.M, Guerguis S., Blevins P. T, Cheshenko N, Gao W., Anastos K., (2022). Failure of Herpes Simplex Virus Glycoprotein D Antibodies to Elicit Antibody-Dependent Cell-Mediated Cytotoxicity: Implications for Future Vaccines, *The Journal of Infectious Diseases*. 226 (9):1489–1498,
- Mahyar H., Hasheminezhad R. & Stanley H (2019) Compressive closeness in networks. *Applied Network Science*. 4(100) <https://doi.org/10.1007/s41109-019-0213-5>
- Maithri G., Manasa B., Vani S.S., Narendra A., Harshita T (2016) Computational Drug Design and Molecular Dynamic Studies-A Review. *International Journal Biomedical Data Mining*; 6: 123. DOI: [10.4172/2090-4924.1000123](https://doi.org/10.4172/2090-4924.1000123)
- Markossian S., Grossman A., Brimacombe K., et al. (2004). Assay Guidance Manual. *Eli Lilly and Company and the National Centre for Advancing Translational Sciences*. <https://www.ncbi.nlm.nih.gov/books/NBK53196/>
- Maslehat S., Sardari S. and Arjenaki G.M (2018). Frequency and Importance of six functional groups that play a role in drug discovery. *Biosciences Biotechnology Research Asia*. 15(3): 541-548. <http://dx.doi.org/10.13005/bbra/2659>
- Meng X.Y., Zhang H.X., Mezei M., Cui M. (2011) Molecular docking: a powerful approach for structure-based drug discovery. *Curr Comput Aided Drug Des*. 7(2):146-57. doi: [10.2174/157340911795677602](https://doi.org/10.2174/157340911795677602). PMID: 21534921; PMCID: PMC3151162.

- Morris G. M. and Lim-Wilby M. (2008) Molecular Modeling of Proteins: Molecular docking. *Methods in Molecular Biology*. 365-382. doi: [10.1007/978-1-59745-177-2_19](https://doi.org/10.1007/978-1-59745-177-2_19) PMID: 18446297.
- Muhammed J., Khan A., Ali A., Fang L., Yanjing W. Xu Q., et al., (2018). Network Pharmacology: Exploring the Resources and Methodologies. *Current Topics in Medicinal Chemistry*. 18 (12): 949-964.
<http://dx.doi.org/10.2174/1568026618666180330141351>
- Muylaert I., Tang K.W. and Elias P. (2011). Replication and recombination of herpes simplex virus DNA. *Journal of Biological Chemistry*. 6;286(18):15619-24. doi: [10.1074/jbc.R111.233981](https://doi.org/10.1074/jbc.R111.233981). PMID: 21362621; PMCID: PMC3091170
- National AIDS and STI Control Programme (Kenya) (2009). Kenya AIDS indicator survey; KAIS 2007: Final Report
http://guidelines.health.go.ke:8000/meia/KAIS_2007_Final.pdf
- Neelabh, Jeswara K. K., Kumari A., Singh K. (2015). *In-silico* designing of NKK: A better ligand than Aciclovir against Herpes Simplex Virus. *Indian Journal. Pharmaceutical and Biological Research*; 3(1):48-55.
- Neves J.B., Braga C.R., Filho C.C., Filho M.T.J., Muratov N.E and Andrade H.C (2018) QSAR- based virtual screening: Advances and Applications in Drug Discovery. *Frontiers in Pharmacology*. 9. <https://doi.org/10.3389/fphar.2018.01275>
- Nunez B.D., Sanahuja C.M., Gallego M.S. and Herranz M.I (2021). Neurotoxicity associated with acyclovir and valacyclovir: A systematic review of cases. *Journal of Clinical Pharmacy and Therapeutics*.46(4):918-926. <https://doi.org/10.1111/jcpt.13464>
- O'Boyle N.M., Banck M., James C.A, Morley C, Vandermeersch T, and Hutchison G. R. (2011) Open Babel: An open chemical toolbox." *Journal of Cheminformatics*. 3(33). DOI:[10.1186/1758-2946-3-33](https://doi.org/10.1186/1758-2946-3-33)
- Oldham S., Fulcher B., Parkes L., Arnatkeviciute A., Suo C., Fornito A. (2019) Consistency and differences between centrality measures across distinct classes of networks. *PLoS ONE* 14(7): e0220061. <https://doi.org/10.1371/journal.pone.0220061>

- Pettersen E.F, Goddard T.D., Huang C.C., Couch G.S., Greenblatt D.M., Meng E.C., et al. (2004) UCSF Chimera-a visualization system for exploratory research and analysis. *Journal of Computational Chemistry*. 25(13):1605-1612.
- Pimentel S. A., Guimarães R. C., and Yifat M. (2013). Molecular Modelling: Advancements and Applications. *Journal of Chemistry*. Article ID 875478, 2 pages <http://dx.doi.org/10.1155/2013/875478>
- Pinder M. and Wright A. (2014). Valaciclovir versus aciclovir for the treatment of primary genital herpes simplex: a cost analysis. *International Journal of STD and AIDS*.26(13):971-973.<https://doi.org/10.1177/0956462414563628>
- Remco P.H.P., Chico M. R., Rowley J. and Low N. (2022). Estimating the global burden of sexually transmitted infections. *The Lancet Infectious Diseases*. 22(8): 1112-1113. [https://doi.org/10.1016/S1473-3099\(22\)00415-7](https://doi.org/10.1016/S1473-3099(22)00415-7)
- Reyes A, Farías A. M, Corrales N., Tognarelli E., González A. P. (2021). Herpes Simplex Viruses Type 1 and Type 2 Infection and Immunity, Reference Module in Biomedical Sciences. Elsevier. <https://doi.org/10.1016/B978-0-12-818731-9.00062-8>
- Rice S.A. (2021). Release of HSV-1 Cell-Free Virions: Mechanisms, Regulation, and Likely Role in Human-Human Transmission. *Viruses*. 2021 Nov 30;13(12):2395. doi: [10.3390/v13122395](https://doi.org/10.3390/v13122395). PMID: 34960664; PMCID: PMC8704881.
- Sabe T.V., Ntombela T., Jhamba A. L., Maguire M.E.G, Govender T, Naicker T, et al. (2021) Current trends in computer aided drug design and highlight of drugs discovered via computational techniques: review. *European Journal of Medicinal Chemistry*. <https://doi.org/10.1016/j.ejmech.2021.113705>
- Sadowski A. L, Upadhyay R., Greelay W. Z., and Margulies J. B. (2021). Current drugs to treat infections with herpes simplex viruses-1 and -2. *Viruses*, 13:1228. <https://doi.org/10.3390/v13071228>
- Salmaso V. and Moro S (2018). Bridging molecular docking to molecular dynamics in exploring ligand-protein recognition process: an overview. *Frontiers in Pharmacology*. doi: [10.3389/fphar.2018.00923](https://doi.org/10.3389/fphar.2018.00923)

- Schiffer J.T., Abu-Raddad L., Mark K.E., Zhu J., Selke S., Magaret A., Wald A., Corey L. (2009). Frequent release of low amounts of herpes simplex virus from neurons: results of a mathematical model. *Sci Transl Med.* 18;1(7):7ra16. [doi: 10.1126/scitranslmed.3000193](https://doi.org/10.1126/scitranslmed.3000193). PMID: 20161655; PMCID: PMC2818652.
- Sehrawat S., Kumar D., and Rouse T. B. (2018). Herpesviruses: Harmonious pathogens but relevant cofactors in other diseases. *Frontiers in Cellular and Infection Microbiology.* 8: [doi: 10.3389/fcimb.2018.00177](https://doi.org/10.3389/fcimb.2018.00177)
- Selvaraj C., Dinesh D.C., Panwar U., Abhirami R., Boura E. and Singh S.K. (2020). Structure-based virtual screening and molecular dynamics simulation of SARS-CoV-2 Guanine-N7 methyltransferase (nsp14) for identifying antiviral inhibitors against COVID-19. *Journal of Biomolecular Structure and Dynamics* 39: 4582–4593. <https://doi.org/10.1080/07391102.2020.1778535>
- Siegel L.R., Miller D. K, and Jemal A. (2019). Cancer Statistics. A Cancer Journal for Clinicians. <https://doi.org/10.3322/caac.21551>
- Schiffer J.T., Corey L. (2013). Rapid host immune response and viral dynamics in herpes simplex virus-2 infection. *Nature Medicine.*;19:280-90. [doi: 10.1038/nm.3103](https://doi.org/10.1038/nm.3103) PMID: 23467247; PMCID: PMC3981536.
- Shannon P., Markiel A., Ozier O., Baliga N.S., Wang J.T., Ramage D., et al. (2003) Cytoscape: a software environment for integrated models of biomolecular interaction networks. *Genome Research* ;13(11):2498-2504. [doi: 10.1101/gr.1239303](https://doi.org/10.1101/gr.1239303). PMID: 14597658; PMCID: PMC403769.
- Shapovalov M.S and Dunbrack R.L Jr (2011) A smoothed Backbone Dependent Rotamer library derived from Adaptive Kernel Density Estimates and Regressions Structure. 19:844-858. [doi: 10.1016/j.str.2011.03.019](https://doi.org/10.1016/j.str.2011.03.019) PMID: 21645855; PMCID: PMC311841
- Sharma D., Sharma S., Akojwar N., Dondulkar A., Yenorkar N., Pandita, D., et al. (2023). An Insight into Current Treatment Strategies, Their Limitations, and Ongoing Developments in Vaccine Technologies against Herpes Simplex Infections. *Vaccines.* 11(206). <https://doi.org/10.3390/vaccines11020206>

- Sliwoski G., Kothiwale S., Meiler J., Lowe E.W. Jr (2014). Computational methods in drug discovery. *Pharmacological Reviews*. 66(1):334-95. doi: [10.1124/pr.112.007336](https://doi.org/10.1124/pr.112.007336)
- Somayeh P., Sunseri J. and Koes R. D. (2016). Open-source molecular modeling. *Journal of Molecular Graphics and Modelling*; 69:127-143. doi: [10.1016/j.jmgm.2016.07.008](https://doi.org/10.1016/j.jmgm.2016.07.008) PMID: 27631126; PMCID: PMC5037051.
- Strick L.B., Wald A. and Celum C. (2006). Management of herpes simplex virus type 2 infection in HIV type 1-infected persons. *Clinical Infectious Disease*. 1;43(3):347-56. doi: [10.1086/505496](https://doi.org/10.1086/505496). PMID: 16804851.
- Su G., Morris J. H., Demchak B., Bader G. D. (2014). Biological network exploration with Cytoscape 3. *Current Protocols Bioinformatics*. 8; 47:8.13.1-24. doi: [10.1002/0471250953.bi0813s47](https://doi.org/10.1002/0471250953.bi0813s47) PMID: 25199793; PMCID: PMC4174321.
- Tripathi A. and Bankaitis V.A. (2017). Molecular Docking: From Lock and Key to Combination Lock. *Journal of Molecular Medicine and Clinical Applications*. 2(1):10.16966/2575-0305.106. doi: [10.16966/2575-0305.106](https://doi.org/10.16966/2575-0305.106) PMID: 29333532; PMCID: PMC5764188.
- Trott O. and Olson A. J. (2010) Autodock Vina: Improving the speed and accuracy of docking with a new scoring function, efficient optimization and multithreading, *Journal of Computational Chemistry*. 31(2): 455–461. doi: [10.1002/jcc.21334](https://doi.org/10.1002/jcc.21334) PMID: 19499576; PMCID: PMC3041641.
- Virgin H.W. (2014). The virome in mammalian physiology and disease. *Cell*. 27;157(1):142-50. doi: [10.1016/j.cell.2014.02.032](https://doi.org/10.1016/j.cell.2014.02.032). PMID: 24679532; PMCID: PMC3977141.
- Wagner, E. K., Sandri-Goldin, R. M. (2008). Herpes simplex viruses: molecular biology. *Encyclopedia of Virology*. Cambridge Academic Press Inc.Cambridge.397–405.
- Wang J., Wang W., Kollman P.A. and Case D.A (2006) Automatic atom type and bond type perception in molecular mechanical calculations. *Journal of Graphics*

and Modelling 25 (2):247-260. doi: [10.1016/j.jmgm.2005.12.005](https://doi.org/10.1016/j.jmgm.2005.12.005) PMID: 16458552.

Wang J., Yuan S., Zhu D., Tang H., Wang N., Chen W., et al. (2018). Structure of the herpes simplex virus type 2 C capsid with capsid-vertex-specific component. *Nature Communications*; 9:3668. <https://doi.org/10.1038/s41467-018-06078-4>

Wang T., Wu M. B., Zhang R. H., Chen Z. J., Hua C., Lin J. P., et al. (2016). Advances in computational structure-based drug design and application in drug discovery. *Current Topics Medicinal Chemistry*. 16: 901–916. <https://doi.org/10.2174/1568026615666150825142002>

Watson A. W., Rhodes J. N., Echenique A. I., Angarone P. M. and Scheetz H. M. (2017). Resolution of acyclovir associated neurotoxicity with the aid of improved estimates using Bayesian approaches: a case report and review of literature. *Journal Clinical Pharmacy and Therapeutics*.42(3):350-355. DOI: [10.1111/jcpt.12520](https://doi.org/10.1111/jcpt.12520)

Wertheim J.O., Smith M.D., Smith D.M., Scheffler K. and Kosakovsky P.SL. (2014). Evolutionary origins of human herpes simplex viruses 1 and 2. *Molecular Biology Evolution*. 31(9):2356-64. doi: [10.1093/molbev/msu185](https://doi.org/10.1093/molbev/msu185)

Whitley R. J. (1996). Herpesviruses. In: Baron S., Editor. *Medical Microbiology*. 4th edition. Galveston, Texas. Chapter 68. <https://www.ncbi.nlm.nih.gov/books/NBK8157/>

Whitley R., Kimberlin D.W., Prober C.G. (2007). Pathogenesis and disease. In: Arvin A, Campadelli-Fiume G, Mocarski E, et al., editors. *Human Herpesviruses: Biology, Therapy, and Immunoprophylaxis*. Cambridge: Cambridge University Press. Chapter 32. <https://www.ncbi.nlm.nih.gov/books/NBK47449/>

Whitley R. and Baines J. (2018). Clinical management of herpes simplex virus infections: past, present and future. *F1000 Research*. <https://doi.org/10.12688/f1000research.16157.1>


- Workowski K.A. and Bolan G.A. (2015). Centers for Disease Control and Prevention. Sexually transmitted diseases treatment guidelines. Diseases Characterized by genital, anal, or perianal ulcers: Genital HSV infections.;64(No. RR-3):1-137. <https://www.cdc.gov/std/tg2015/herpes.html>
- World Health Organization (2016). WHO guidelines for the treatment of herpes simplex virus. Geneva, Switzerland ISBN 978 92 4 154987 5.
- Wu Y. and Wang G. (2018) Machine Learning Based Toxicity Prediction: From Chemical Structural Description to Transcriptome Analysis. *International Journal of Molecular Sciences*;19(8): 2358. doi: [10.3390/ijms19082358](https://doi.org/10.3390/ijms19082358) PMID: 30103448; PMCID: PMC6121588.
- Xu J. and Zhang Y. (2010). How significant is a protein structure similarity with TM-score =0.5? *Bioinformatics*. 7:889–895. <https://doi.org/10.1093/bioinformatics/btq066>
- Xu Q., Fan Q. and Olavi P. (2012). Network Pharmacology and Traditional Chinese Medicine. *Journal of Traditional and Complementary Medicine*.4(1):1–7. <http://dx.doi.org/10.5772/53868>
- Yang H., Lou C., Sun L., Li J., Cai Y., Wang Z., Li W., Liu G. and Tang Y. (2019) AdmetSAR 2.0: web-service for prediction and optimization of chemical ADMET properties. *Bioinformatics*. 35(6):1067-1069. <https://doi.org/10.1093/bioinformatics/bty707>.
- Yang J, Anishchenko I, Park H, Peng Z., Ovchinnikov S. and Baker D. (2020). Improved protein structure prediction using predicted interresidue orientations, *PNAS*, 117: 1496-1503. <https://doi.org/10.1073/pnas.1914677117>
- Zhang G-B, Li Q-Y, Chen Q-L, and Su S-B (2013). Network Pharmacology: A New Approach for Chinese Herbal Medicine Research *Hindawi*; 621423:9 pages. <https://doi.org/10.1155/2013/621423>
- Zhang Q-Y, Mao X., Guo Y-Q, Lin N. and Li S. (2016). Network pharmacology-based approaches capture essence of Chinese Herbal Medicines. *Chinese Herbal Medicines*. 8(2):107-116. [https://doi.org/10.1016/S1674-6384\(16\)60018-7](https://doi.org/10.1016/S1674-6384(16)60018-7)

- Zhu S. and Borbolla V. A. (2021). Pathogenesis and virulence of herpes simplex virus, *Virulence*, 12(1):2670-2702, DOI: [10.1080/21505594.2021.1982373](https://doi.org/10.1080/21505594.2021.1982373)
- Zinser E., Krawczyk A., Mühl-Zürbes P., Aufderhorst U., Draßner C., Stich L., et al. (2018). A new promising candidate to overcome drug resistant herpes simplex virus infections. *Journal of Antiviral Research*. 149:202-210. <https://doi.org/10.1016/j.antiviral.2017.11.012>


APPENDICES

Appendix I: Research Publication


Scientific African 19 (2023) e01461


ELSEVIER

Contents lists available at ScienceDirect
Scientific African
journal homepage: www.elsevier.com/locate/sciaf



In silico investigation of acyclovir derivatives potency against herpes simplex virus



Clive M. Nyaribo*, Florence A. Ng'ong'a, Steven G. Nyanjom

Department of Biochemistry, School of Biomedical Sciences, College of Health Sciences, Jomo Kenyatta University of Agriculture and Technology, PO Box 62000-00200, Nairobi, Kenya

ARTICLE INFO

Article history:
Received 20 June 2022
Revised 13 November 2022
Accepted 22 November 2022

Editor name: DR B Gyampoh

Keywords:
Computer aided drug design
Network pharmacology
Molecular docking
Acyclovir derivatives
Herpes simplex virus

ABSTRACT

Herpes simplex virus (HSV) is a major human pathogen, sub-divided into two types: HSV-1 which causes oral and perioral infections and HSV-2 which causes genital herpes. The global disease burden is high with 67% and 11% of the World's population being infected with HSV-1 and HSV-2 respectively. Acyclovir, an FDA approved drug, is a synthetic purine nucleoside analogue used for the treatment of HSV infections. The drug acts via the viral encoded thymidine kinase and competitively inhibits viral DNA polymerase. Emerging HSV resistance to acyclovir and lack of approved vaccines necessitates need for effective strategies to circumvent the viral infection. Derivatives of acyclovir were modelled using computer aided drug design techniques through Chemskech and drugability determined based on Lipinski's Ro5 where a Python filtering code was created and derivatives with zero non-violations were selected. Putative biological targets were determined through network pharmacology and validated through gene ontology. Molecular docking with known and putative targets was done to determine the binding affinities of the acyclovir derivatives. Based on enzyme inhibition scores, pharmacokinetics prediction was done on Molinspiration while pharmacodynamics predictions were done on AdmetSAR based on bioavailability scores. Thirty acyclovir derivatives were modelled of which 22 had zero non-violations. 2-[(3, 6-dihydro-9H-purin-9-yl)methoxy]ethan-1-ol had the highest enzyme inhibition score at 1.0 compared to 0.84 for acyclovir. The molecule was further optimized generating (2-[(6-methyl-6,9-dihydro-3H-purin-9-yl)methoxy]ethan-1-ol) which had a better bioavailability and a higher blood brain barrier value of 0.9880 indicating possible better patient tolerance. 2-[(6-methyl-6,9-dihydro-3H-purin-9-yl)methoxy]ethan-1-ol had an enzyme inhibition score of 0.90 and binding energies of -5.1 kcal/mol when docked against thymidine kinase. The intra-viral HSV PPI network was analysed and DNA replication helicase (UL5) and serine/threonine-protein kinase (US3) were selected due to functional similarity with thymidine kinase with kappa statistics value of 0.30 and 0.24 respectively. Gene enrichment analysis indicated that the biological targets UL5 and US3 had a significant P value of 0.62 based on Benjamin Correction at P<0.05. The study recommends *in vitro* and *in vivo* validation of this novel compound and molecular validation of the two new potential biological targets for possible development of new anti-herpes therapeutic compounds.

© 2022 The Author(s). Published by Elsevier B.V. on behalf of African Institute of Mathematical Sciences / Next Einstein Initiative.
This is an open access article under the CC BY-NC-ND license (<http://creativecommons.org/licenses/by-nc-nd/4.0/>)

* Corresponding author.
E-mail address: clivenyaribo@gmail.com (C.M. Nyaribo).

<https://doi.org/10.1016/j.sciaf.2022.e01461>
2468-2276/© 2022 The Author(s). Published by Elsevier B.V. on behalf of African Institute of Mathematical Sciences / Next Einstein Initiative. This is an open access article under the CC BY-NC-ND license (<http://creativecommons.org/licenses/by-nc-nd/4.0/>)

Introduction

Herpes simplex Virus (HSV) is an enveloped, double stranded DNA virus in the *Herpesviridae* family and *Simplex virus* genus [11]. HSV-1 causes oral and perioral herpes, which is highly contagious while HSV-2 causes genital and anal herpes, which is of particular concern due to its epidemiological synergy with HIV infection and transmission [12]. The infections are mainly asymptomatic but can cause mild to severe symptoms which include skin blisters and lesions on mucous membranes and genitals, fever during clinical episodes and headache [10]. The global prevalence of HSV-1 and HSV-2 is 67% and 11% respectively [19] with Africa accounting for 32% of the HSV infections [20]. Kenyan adults have a higher HSV-2 prevalence rate of 26.6% [3].

FDA approved drugs; acyclovir, valaciclovir and famciclovir which are purine nucleosides, are used for the treatment of HSV infections. The mode of action for the drugs involves monophosphorylation by the HSV-encoded thymidine kinase (TK) in the virally infected cells [17]. Famciclovir and valaciclovir averagely cost 6.20 USD and 3.24 USD per unit respectively compared to acyclovir which costs 2.19 USD, thus treatment using acyclovir is cheaper [26]. Side effects such as neurotoxicity and nausea have been reported with the use of valaciclovir [7] and famciclovir [13] respectively, and Acyclovir is preferred for the treatment of recurrent clinical episodes of genital HSV infection due to its lower price, tolerability and safety [4]. Acyclovir is converted by HSV-encoded thymidine kinase into acyclovir monophosphate which is further converted to acyclovir diphosphate by cellular guanylate kinase and into triphosphate by a number of cellular enzymes. Acyclovir triphosphate competes for endogenous deoxyguanosine triphosphate (dGTP) and therefore competitively inhibits viral DNA polymerase. It is also incorporated into viral DNA, where it acts as a chain terminator because of the lack of 3'-hydroxyl group. The terminated DNA template containing acyclovir binds DNA polymerase and leads to its irreversible inactivation [16].

There is emergence of acyclovir drug resistant HSV especially in immunocompromized patients who require long-term anti-HSV therapy due to recurrent clinical episodes of HSV infections [41]. This is caused by mutation on viral thymidine kinase and DNA polymerase genes. The HSV-1 and HSV-2 elicit lifelong infection and evade the host's immediate antiviral response [27]. Currently there is no approved vaccine for the prevention of HSV infection [21]. Severe conditions such as, neurotoxicity especially occur when acyclovir is taken with zidovudine, an HIV regimen drug [36].

There is a need to design and develop new drug compounds and identify new targets and compounds against HSV to circumvent drug resistance. In this study, molecular modelling was used to design acyclovir derivatives. Network pharmacology was used to identify new putative drug targets from an HSV intraviral protein-protein interaction (PPI) network. Molecular docking was used for virtual screening of the derivatives. Pharmacodynamics and pharmacokinetics of the acyclovir derivatives were determined to elucidate bioavailability and bioactivity.

Methodology

Molecular modelling

The Simplified Molecular-Input Line-Entry System (SMILES) format of acyclovir was obtained from Drug Bank (<https://www.drugbank.ca/>). Chemscketch software version 12.1.0.31258 was used to model the acyclovir derivatives and provide IUPAC nomenclature [1]. The Acyclovir SMILES notation was pasted on Chemscketch and the molecule manipulated on a two-dimensional space. Ligand based drug design was used to model the acyclovir derivatives. The acyclovir functional group was manipulated using Chemscketch functions to design 30 acyclovir derivatives. Open Babel version 2.4.1 was used to convert the acyclovir derivatives to MDL Mol [23]. The derivatives were evaluated for druglikeness.

Drugability or druglikeness of the acyclovir derivatives was evaluated using Lipinski's Rule of Five to select acyclovir derivatives presumed to be biologically active compounds and filter out the non-drug like molecules [8,33]. MarvinSketch, version 19.17, was used to calculate the molecular descriptors of the parent drug, acyclovir and the designed derivatives using the chemoinformatics plugins [9]. Sub setting and filtering code was written in Python version 3.9.7 [34].

Network pharmacology

PPI data was downloaded from HVInt 2.0 Database (<http://topf-group.ismb.lon.ac.uk/hvint/>) with the confidence intervals of the interactions ranging from 0.147 to 0.972 including both experimentally supported and computationally predicated interactions [5]. The data was mapped from Uniprot accession numbers to open reading frames using HVInt 2.0 Database and validated using Uniprot Mapping/Retrieval Tool.

Cytoscape 3.0 was used for network construction, visualization and topological analysis [29,32]. Undirected PPI network was created by importing the HSV Proteins interaction data into Cytoscape and assigning the columns appropriately, whereby column A was assigned as the source node, column B as the target node and the confidence scores as the edge attribute. Network editing was done by removing self-nodes, 1 unconnected node and 5 single connected nodes. Network analyser was used to analyse the network's local topological attributes and node size was mapped based on degree and edge size mapped based on confidence score. CytoNCA was used to calculate centrality measures of the HSV structural proteins PPI unweighted network; Eigenvector, Local average connectivity (LAC). Closeness centrality (CC) and Betweenness central-

ity (BC) [24]. Python 3 was used to rank the nodes to identify a focal node as a presumed biological drug target that can effectively transfer drug effects to its immediate neighbours and affect distant neighbours via indirect routes.

The Database for Annotation, Visualization and Integrated Discovery (DAVID; <https://david.ncifcrf.gov/>), was used for GO annotation of the selected targets. The selected nodes were uploaded on the search panel including thymidine kinase (UL23). Using Kappa statistics, the functional similarity between the selected nodes and UL23 was calculated with the Kappa threshold set at $K > 0.20$ [31], the gene list and population background being HSV-1. The semantic similarity of the targets selected to HSV-2 was also calculated since acyclovir can be used for the treatment of both HSV-1 and HSV-2. Gene enrichment analysis was performed through functional annotation clustering based on Benjamin Correction at $P < 0.05$.

Protein modelling

The known acyclovir target, thymidine kinase was downloaded from Protein Data Bank (<https://www.rcsb.org/>) and stored in PDB structure format. The 3D protein structures of the helicase primase complex and serine/threonine protein kinase were predicted using trRosetta [40] since the proteins were lacking homologs on Protein Data Bank. De novo modelling was used for protein structure prediction. Amino acid sequences were obtained from Uniprot (<https://www.uniprot.org/>) in fasta format. The sequences were submitted separately to the trRosetta server (<https://yanglab.nankai.edu.cn/trRosetta/>). The trRosetta workflow involve deep residual neural network application to predict the inter-residue distance and orientation distribution which are converted into smooth restraints and the restraints guide Rosetta to build 3D structure models based on energy minimizations [14]. The models obtained were subjected to evaluation based on the template modelling (TM) score which is based on probability of the top predicted distance and the convergence of the top models. TM scores are between 0 and 1, scores below 0.17 correspond to randomly chosen unrelated proteins whereas structures with a score higher than 0.5 assume generally the same fold in SCOP/CATH databases [38].

Molecular docking

Molecular docking was used to predict the preferred relative orientations of the acyclovir derivatives in the receptor (Target) active sites (Khanna et al., 2019). Protein-ligand docking was used [2]. Autodock Vina version 1.1.2 which uses united atom scoring function and Broyden-Fletcher-Goldfarb-Shanno (BFGS) algorithm for local optimization was used for molecular docking [35]. Chimera version 1.13.1 which is an integrative graphical tool was used for generating input files for Autodock Vina through ligand, receptor preparation and coordinate setting [25].

Solvent molecules were deleted from the receptors and for thymidine kinase the ligand was selected and deleted from the complex. Gasteiger charges and polar hydrogen atoms that are Sybl atom type were added to the receptors with Amber force field parameters. Incomplete side chains were replaced using Dunbrack 2010 rotamer library [30]. Ligand preparation involved addition of hydrogen atoms and charges using the Add Charge Tool which is a call to Antechamber, [37]. The charge method used was semi-empirical with bond charge correction (AM1BCC). Grid box coordinates for docking were set as follows X centre = 31, Y centre = 24 and Z centre = 44. The size points search base were set as X = 22, Y = 24 and Z = 28. During docking number of binding modes were set at 10, search exhaustiveness was set at 8 to attain global minimum.

Quantitative structure-activity relationship (QSAR)

The Molinspiration Bioactivity Predictor (<https://www.molinspiration.com/>) calculated enzyme inhibition scores for 16 acyclovir derivatives including the acyclovir drug by pasting the SMILES files of the molecules to the text window. AdmetSAR 2.0 (<http://lmmd.ecust.edu.cn/admetSar1/>) was used to generate the bioavailability scores for cell permeability (Caco2), blood brain barrier (BBB), human intestinal absorption (HIA) and P- glycoprotein substrate [39].

Results

Molecular modelling

Thirty acyclovir derivatives were modelled and based on Lipinski's Ro5; 22 (73%) had zero non-violations (Fig. 1). The corresponding IUPAC names are indicated in Table 1.

Network pharmacology

The PPI network consisted of 65 nodes and 377 edges hence highly connected (Fig. 2). The average degree was 11 meaning an individual node is connected to a fairly high number of edges. The mean shortest path length was 2.024 which is fairly low suggesting the nodes are functionally related (Table 2).

Top 10% ranking was done based on local topological attributes and centrality measures (Tables 3 and 4). Based on the four centrality measures; - EC, BC, CC and IAC, 11 non-repetitive protein nodes were obtained after ranking: UL40, UL15, UL31, UL21, UL32, UL35, UL34, UL46, UL49, UL33 and UL14.

Table 1
Key indicating derivative number and IUPAC name.

Derivative Number	IUPAC Name
Acyclovir	2-amino-9-[(2-hydroxyethoxy)methyl]-3,9-dihydro-6H-purin-6-one
1	2-[(2-amino-6-methylidene-3,6-dihydro-9H-purin-9-yl)methoxy]ethan-1-ol
2	2-[(2-amino-6-imino-3,6-dihydro-9H-purin-9-yl)methoxy]ethan-1-ol
3	9-(ethoxymethyl)-6-methylidene-6,9-dihydro-3H-purin-2-amine
4	5-amino-3-[(2-hydroxyethoxy)methyl]imidazo[4,5-e][1,3]oxazin-7(3H)-one
6	2-amino-9-(ethoxymethyl)-3,9-dihydro-6H-purin-6-one
7	2-hydroxy-9-[(2-hydroxyethoxy)methyl]-3,9-dihydro-6H-purin-6-one
8	methyl 4-[(2-amino-6-oxo-3,6-dihydro-9H-purin-9-yl)methoxy]butaneperoxoate
11	(1 <i>Z</i> ,5 <i>Z</i>)-6-amino-3-[(2-hydroxyethoxy)methyl]-3,4,5,9-tetrahydro-8 <i>H</i> -1,3,5,7-tetrazonin-8-one
12	2-amino-3,9-dihydro-6H-purin-6-one
14	5-amino-3-[(2-hydroxyethoxy)methyl]-3 <i>H</i> ,4 <i>H</i> ,5 <i>H</i> ,6 <i>H</i> ,7 <i>H</i> -imidazo[4,5- <i>b</i>]pyridin-7-one
15	2-amino-9-[(1 <i>Z</i>)-3-(methylamino)prop-1-en-1-yl]-3,9-dihydro-6H-purin-6-one
16	2-amino-8-benzyl-9-[(2-hydroxyethoxy)methyl]-3,9-dihydro-6H-purin-6-one
17	2-[(3,6-dihydro-9 <i>H</i> -purin-9-yl)methoxy]ethan-1-ol
18	5-amino-3-[(2-methoxyethoxy)methyl]-3,4-dihydro-7 <i>H</i> -pyrrolo[2,3- <i>c</i>]pyridin-7-one
19	1-(hydroxymethyl)-1,7-dihydro-4 <i>H</i> -imidazo[4,5- <i>c</i>]pyridin-4-one
20	9-(ethoxymethyl)-6,9-dihydro-3 <i>H</i> -purin-2-amine
24	2-[(2-amino-6-oxo-3,6-dihydro-9 <i>H</i> -purin-9-yl)methoxy]ethyl 3-methylbutanoate
25	9-[(2-(3-methylbutoxy)ethoxy)methyl]-6,9-dihydro-3 <i>H</i> -purine
27	2-amino-9-[(2-hydroxyethoxy)methyl]-3,9-dihydro-6H-purin-6-one
28	2-[(4-[(<i>E</i>)-aminomethylidene]carbamoyl)-1 <i>H</i> -imidazol-1-yl)methoxy]ethyl propanoate
29	2-amino-9-benzyl-3,9-dihydro-6H-purin-6-one
30	9-benzyl-6,9-dihydro-3 <i>H</i> -purin-2-amine

Table 2
Global topological measurements of the HSV PPI network.

Symbol	Description	Value
N	Number of nodes	65
E	Number of edges	377
D	Diameter	4
<K>	Average degree	11.6
Acc	Average clustering coefficient	0.333
Mspl	Mean shortest path length	2.024

Table 3
Top 10% Node Ranking based on Centrality Measures values.

	Eigenvector Centrality		Betweenness Centrality		Closeness Centrality		Local Average Connectivity	
	Node	Value	Node	Value	Node	Value	Node	Value
1.	UL40	0.248725	UL40	440.93887	UL40	0.653051	UL32	8.000000
2.	UL15	0.243497	UL15	376.79822	UL15	0.640000	UL31	7.520000
3.	UL31	0.237283	UL21	284.44037	UL31	0.621359	UL34	7.157895
4.	UL21	0.229737	UL35	250.43700	UL21	0.615385	UL15	6.857143
5.	UL32	0.203523	UL46	225.87611	UL34	0.581818	UL21	6.720000
6.	UL35	0.202714	UL49	208.77910	UL46	0.581818	UL40	6.200000
7.	UL34	0.201134	UL31	168.46600	UL33	0.576577	UL14	6.000000

Table 4
Top 10% Node Ranking based on local Topological Attributes.

S. No.	Neighbourhood Connectivity		Clustering Coefficient		Topological Coefficient		Radicity		Stress	Average Shortest Path Length		Degree		
	Node	Value	Node	Value	Node	Value	Node	Value		Node	Value	Node	Value	
1.	US3	23.0	UL11	1.0	US3	0.70	UL40	0.86	UL40	2178	UL40	1.53	UL40	30
2.	UL11	21.0	US2	0.7	US11	0.65	UL15	0.85	UL15	1902	UL15	1.56	UL15	28
3.	UL3	19.8	UL6	0.6	UL51	0.62	UL31	0.84	UL21	1598	UL31	1.60	UL21	25
4.	UL37	19.4	RL2	0.6	UL6	0.53	UL21	0.84	UL35	1418	UL21	1.62	UL31	25
5.	UL6	19.3	UL5	0.6	UL11	0.50	UL46	0.82	UL46	1314	UL46	1.71	UL46	23
6.	UL32	18.8	UL12	0.6	RL2	0.47	UL34	0.82	UL31	1076	UL34	1.71	UL35	23
7.	UL22	18.7	UL37	0.4	UL52	0.42	UL33	0.81	UL49	1026	UL33	1.73	UL33	21

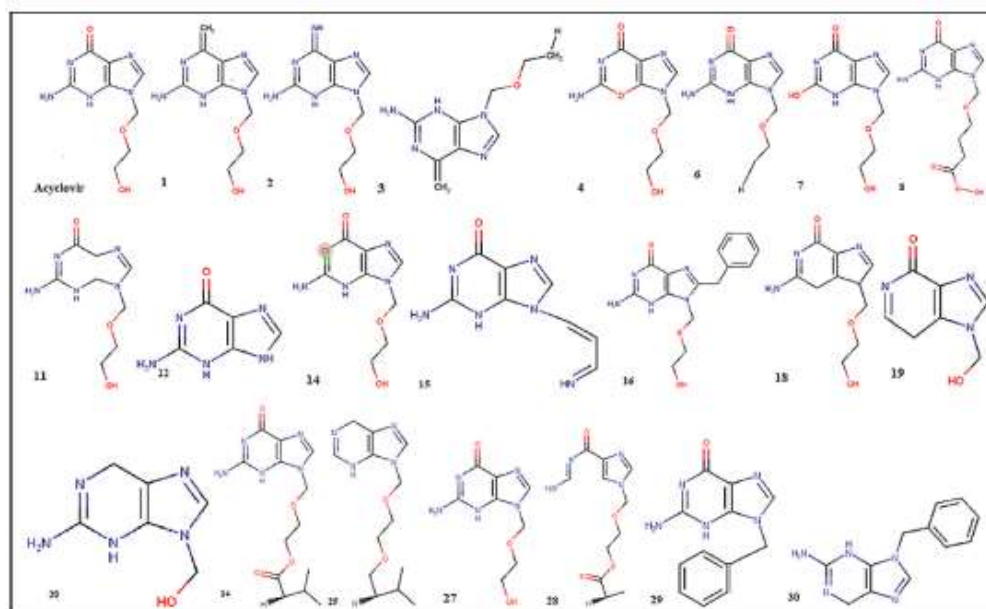


Fig. 1. Acyclovir derivatives filtered based on Lipinski's Ro5.

The nodes obtained were the most focal in the network in terms of eccentricity and modularity. Based on neighbourhood connectivity, topological and clustering coefficients, radiality, average shortest path length, stress and degree 13 nodes protein nodes were obtained; US3, US11, UL51, UL6, UL11, RL2, UL52, US2, UL5, UL12, UL37, UL3 and UL22.

DNA replication helicase (UL5) and serine/threonine protein kinase (US3) were selected as presumed putative biological targets for acyclovir derivatives based on functional similarity with thymidine kinase (UL23) (Table S1). ATP binding and nucleotide binding were selected as enriched terms since they are associated with the acyclovir mechanism of action and related genes included UL5 and US3 with significant P value of 0.62 based on Benjamin Correction at $P < 0.05$.

Protein modelling

The best predicted model for Serine/Threonine Protein kinase (US3) had a TM score of 0.543 while that for DNA replication helicase (UL5) had a TM score of 0.194. Fig. S1 illustrate the 3D best models for (a) DNA replication helicase and (b) serine/threonine protein kinase (b).

The Ramachandran plots for omega, theta and phi torsion angles are illustrated on Figs. S2 and S3 for DNA replication helicase and serine/threonine protein kinase respectively.

Molecular docking

2-amino-9-[(2-hydroxyethoxy)methyl]-3,9-dihydro-6H-purin-6-one (1), 2-[(3,6-dihydro-9H-purin-9-yl)methoxy]ethan-1-ol (17) and 1-(hydroxymethyl)-1,7-dihydro-4H-imidazo[4,5-c]pyridin-4-one (19) had binding energies of -4.7 Kcal/mol while 2-amino-9-[(2-hydroxyethoxy)methyl]-3,9-dihydro-6H-purin-6-one (27) had binding energy of -4.8 Kcal/mol when docked against thymidine kinase. When docked against DNA replication helicase, 2-[(3,6-dihydro-9H-purin-9-yl)methoxy]ethan-1-ol (17) had the lowest binding energy at -6.2 Kcal/mol followed by 2-amino-9-[(3Z)-3-(methylimino)prop-1-en-1-yl]-3,9-dihydro-6H-purin-6-one (15) at -6.1 Kcal/mol. 2-amino-9-[(2-hydroxyethoxy)methyl]-3,9-dihydro-6H-purin-6-one (1), 9-(ethoxymethyl)-6-methylidene-6,9-dihydro-3H-purin-2-amine (3) and 1-(hydroxymethyl)-1,7-dihydro-4H-imidazo[4,5-c]pyridin-4-one (19) had binding energy of 3.6 Kcal/mol while 2-[(3,6-dihydro-9H-purin-9-yl)methoxy]ethan-1-ol (17) had binding energy of 3.5 Kcal/mol when docked against serine/threonine protein kinase (Table S2).

As per the mean, minimum and maximum binding energies, DNA replication helicase emerged as the best target (Table S3).

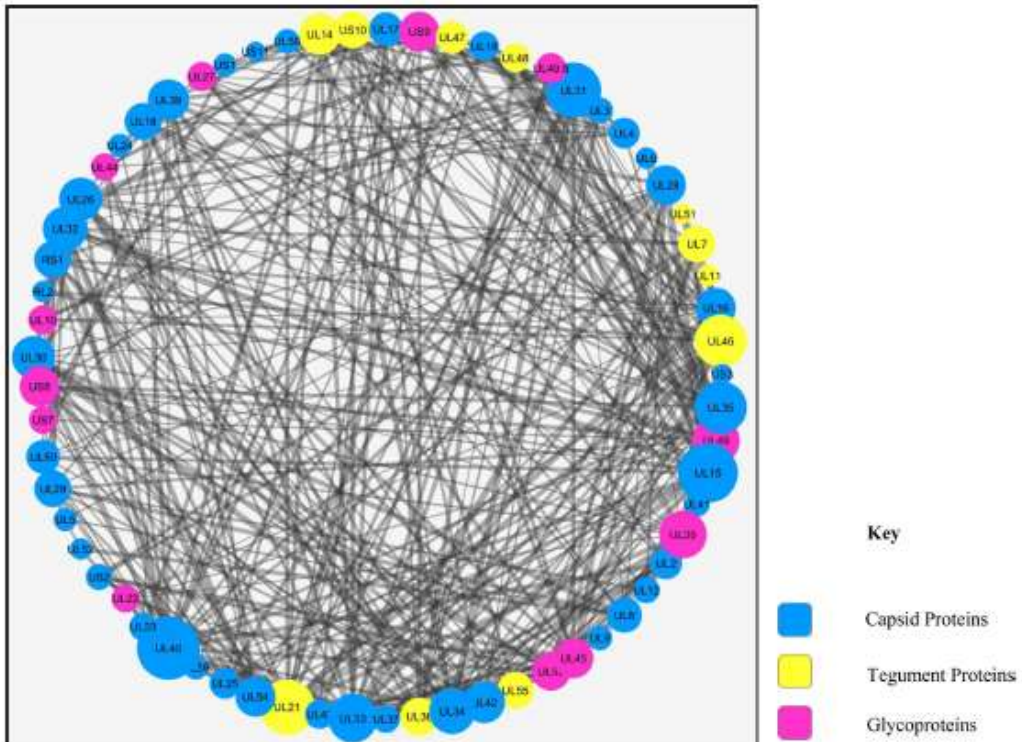


Fig. 2. The HSV PPI Network.

Quantitative structure activity relationship analysis (QSAR)

2-[(3,6-dihydro-9H-purin-9-yl)methoxy]ethan-1-ol (17) had the highest enzyme inhibition score at 1.0 compared to 0.84 for acyclovir (Fig. S4). The enzyme score for 2-[(3,6-dihydro-9H-purin-9-yl)methoxy]ethan-1-ol is consistent with the lowest binding energies of -6.2 Kcal/mol when docked against DNA replication helicase. 2-[(3,6-dihydro-9H-purin-9-yl)methoxy]ethan-1-ol lacks oxygen and amino group present in acyclovir. 2-amino-9-[(3Z)-3-(methylimino)prop-1-en-1-yl]-3,9-dihydro-6H-purin-6-one(15) also had an enzyme inhibition score of 0.98 consistent with binding energies of -6.1 Kcal/mol. Compared to acyclovir, 2-amino-9-[(3Z)-3-(methylimino)prop-1-en-1-yl]-3,9-dihydro-6H-purin-6-one lacks an hydrogen and nitrogen atom on the guanine functional group instead of an hydroxide group.

The bioavailability scores for the lead molecules were fairly good, with 2-amino-9-[(3Z)-3-(methylimino)prop-1-en-1-yl]-3,9-dihydro-6H-purin-6-one (15) having a good human intestinal score of 0.9965 which is higher than acyclovir score of 0.9583. 2-[(3,6-dihydro-9H-purin-9-yl)methoxy]ethan-1-ol (17) had a score of 0.9186 (Fig. S5).

Lead optimization

The lead compounds, 2-[(3,6-dihydro-9H-purin-9-yl)methoxy]ethan-1-ol (17) and 2-amino-9-[(3Z)-3-(methylimino)prop-1-en-1-yl]-3,9-dihydro-6H-purin-6-one (15) were optimized. The optimized lead molecule for 2-[(3,6-dihydro-9H-purin-9-yl)methoxy]ethan-1-ol (17), 2-[(6-methyl-6,9-dihydro-3H-purin-9-yl)methoxy]ethan-1-ol had lower binding energies when docked against thymidine kinase, DNA replication helicase and serine/threonine protein kinase at -5.6 kcal/mol, -4.7 kcal/mol and -4.1 kcal/mol respectively.

The optimized lead molecule for 9-[(3Z)-3-(methylimino)prop-1-en-1-yl]-3,9-dihydro-6H-purin-6-one (15), 2-amino-9-hydroxy-6,9-dihydro-3H-purin-6-one when docked against thymidine kinase, DNA replication helicase and serine/threonine protein kinase had binding energies of -5.1 kcal/mol, -4.5 kcal/mol and -5.1 kcal/mol respectively.

2-[(6-methyl-6,9-dihydro-3H-purin-9-yl)methoxy]ethan-1-ol had an enzyme inhibition score of 0.90 while 2-amino-9-hydroxy-6,9-dihydro-3H-purin-6-one had an enzyme inhibition score of 0.44. Thus, 2-[(6-methyl-6,9-dihydro-3H-purin-9-yl)methoxy]ethan-1-ol was the best optimized lead molecule (Fig. S6).

Discussion

The bioavailability of acyclovir ranges from 10 – 30% with low permeability [6]. Out of thirty modelled derivatives, two derivatives 2-[(3,6-dihydro-9H-purin-9-yl)methoxy]ethan-1-ol and 2-amino-9-[(3Z)-3-(methylimino)prop-1-en-1-yl]-3,9-dihydro-6H-purin-6-one emerged as lead compounds with high bioavailability. Although the lead compounds and Acyclovir are analogs of the same nucleoside, the slight structure differences between the drugs have led to differences in pharmacology including the human intestinal absorption and cell permeability as was observed for Penciclovir (PCV), an anti-HSV guanosine analogue with structural differences with Acyclovir. PCV had higher affinity for HSV TK and viral DNA polymerase as compared to Acyclovir thus higher concentrations over prolonged periods in infected cells [18].

Molecular docking results indicated that DNA replication helicase had the lowest mean binding energies followed by serine/threonine protein kinase thus high bioactivity of the derivatives compared to thymidine kinase as the target. Two derivatives, 2-[(3,6-dihydro-9H-purin-9-yl)methoxy]ethan-1-ol and 2-amino-9-[(3Z)-3-(methylimino)prop-1-en-1-yl]-3,9-dihydro-6H-purin-6-one had lower binding which correlates to the high bioactivity.

The optimized lead compound, 2-[(6-methyl-6,9-dihydro-3H-purin-9-yl) methoxy] ethan-1-ol, has a methyl group and no carbonyl and amine group thus increased bioavailability and bioactivity due to increased topological polar surface area compared to acyclovir which has low cell permeability.

This study developed and optimized a novel acyclovir derivative; 2-[(6-methyl-6,9-dihydro-3H-purin-9-yl) methoxy]ethan-1-ol and went further to evaluate its pharmacodynamics and pharmacokinetics. Similar studies for instance, [22], designed a ligand known as NNK that targeted the thymidine kinase but, they only evaluated binding affinity through molecular docking.

The main basis for HSV resistance to nucleoside analogs resides in mutations in the thymidine kinase gene [28]. Network pharmacology and gene ontology studies identified putative HSV targets, DNA replication helicase (UL5) and serine/threonine protein kinase (US3) to circumvent HSV drug resistance. The predicted proteins provide potential therapeutic targets for anti-herpes drugs that does not necessarily utilize the thymidine kinase directed pathway. The molecular functions: ATP binding and kinase/helicase activity of the putative targets are as a result of helicase motifs which are involved in viral replication. Anti-herpes drugs target to inhibit viral replication thus control and treat herpes simplex virus infections.

Acyclovir is known to cause side effects such as neurotoxicity [36], nausea and vomiting [15]. Blood brain barrier (BBB) prediction of acyclovir derivatives modelled showed values above 0.90 with the optimized lead having a value of 0.9880 thus reduced side effects to the patient. This shall increase tolerance in patients which shall lead to increased adherence to treatment and overall reduced infection.

Global prevalence of HSV infections is high with Africa accounting for a third of the infections. The research tackles herpes simplex virus, a communicable disease that is a challenge to sustainable development as captured under Sustainable Development Goal 3: Good Health and Well-being, with specific target of alleviating infectious diseases including herpes simplex virus infections by 2030. The SDG 3 is in tandem with the African Union's Agenda 2063, priority area-health which seeks to have healthy citizens to ensure a prosperous Africa based on inclusive growth and sustainable development. Kenya's Vision 2030 blueprint outlines healthcare as a social pillar and the Ministry of Health's Kenya National Infection Prevention and Control Policy seeks to strengthen treatment of infectious disease and tackle emerging antimicrobial resistance, which the study tackles.

Conclusions

The identification of two more potential biological targets; DNA replication helicase and serine/threonine protein kinase can be used to introduce polypharmacology in the design and development of novel synergistic drug therapies against herpes simplex virus to circumvent drug resistance. The scientific community can explore the targets identified in development of therapeutic molecules against herpes simplex virus.

The design and development of optimized lead molecule, novel compound (2-[(6-methyl-6,9-dihydro-3H-purin-9-yl)methoxy]ethan-1-ol) can contribute greatly to the management of HSV infections. The in-silico validation of the novel compound in this study underscores the importance of computer aided drug design as an alternative method of drug development.

However, the study recommends further in vitro and in vivo validation of this novel compound (2-[(6-methyl-6,9-dihydro-3H-purin-9-yl)methoxy]ethan-1-ol) and molecular validation of the two new potential biological targets (DNA replication helicase and serine /threonine-protein kinase) for possible development of new anti-herpes therapeutic compounds.

Funding

Japan International Cooperation Agency Grant numbers: Africa-ai-Japan Project Innovation Research Grants Category Two 2020/2021.

Declaration of Competing Interest

The authors declare that they have no known competing financial interests or personal relationships that could have appeared to influence the work reported in this paper.

Supplementary materials

Supplementary material associated with this article can be found, in the online version, at doi:10.1016/j.sciaf.2022.e01461.

References

- [1] Advanced Chemistry Development/ChemSketch Version 2018.2.5, Inc, Toronto, ON, Canada, 2019 www.acdlabs.com.
- [2] J. Ainsley, L. Alessio, J. Adrian, C. Mulholland, Z. Christow, G. Tatyana, Advances in Protein Chemistry and Structural Biology: Combined Quantum Mechanics and Molecular Mechanics Studies of Enzymatic Reaction Mechanisms, 111, Elsevier, 2018, pp. 1–32. VolumePages, doi:10.1016/j.bsapcsb.2018.07.001.
- [3] B. Akinyi, C. Odhiambo, F. Otiemo, S. Itzraule, S. Oswago, E. Kerubo, K. Ndho, Z. Ceh, Prevalence, incidence and correlates of HSV-2 infection in an HIV incidence adolescent and adult cohort study in western Kenya, *PLoS ONE* 12 (6) (2017) e0178907, doi:10.1371/journal.pone.0178907.
- [4] M.D. Álvarez, E. Castillo, F.J. Duarte, J. Arriagada, N. Corrales, A. Mónica, A.H. Farías, A.C. Muñoz, P.A. González, Current antivirals and novel botanical molecules interfering with herpes simplex virus infection, *Front. Microbiol. Virol.* (2020), doi:10.3389/fmicb.2020.00139.
- [5] P. Ashford, A. Hernandez, T.M. Greco, A. Buch, B. Sodeik, I.M. Cristea, K. Gränewald, A. Shepherd, M. Topf, HVint: a strategy for identifying novel protein-protein interactions in herpes simplex virus type, *Mol. Cell. Proteom.* 15 (9) (2016) 2939–2953, doi:10.1074/mcp.M116.058552.
- [6] G.S.M. Assis, F.C.T. Pedrosa, S.F. Moraes, R.G. Pereira, J. Souza, M.L.A. Ruela, Novel insights to enhance therapeutics with acyclovir in the management of herpes simplex encephalitis, *J. Pharmaceut. Sci.* 110 (4) (2021) P1557–P1571. VolumeIssue, doi:10.1016/j.xphs.2021.01.003.
- [7] D. Brandariz-Núñez, M. Correas-Sanahuja, S. Maya-Gallego, Neurotoxicity associated with acyclovir and valacyclovir: a systematic review of cases, *J. Clin. Pharm. Ther.* 46 (2021) 918–926, doi:10.1111/jcpt.13464.
- [8] Z.L. Benet, M.C. Hosey, O. Ursu, T.I. Oprea, BDDCS, the Rule of Five and Drugability, 101, *Advanced Drug Delivery Reviews*, Elsevier, 2016, pp. 89–98, doi:10.1016/j.addr.2016.05.007.
- [9] ChemAxon (2019) MarvinSketch version 19.17 <http://www.chemaxon.com>.
- [10] S. Crimi, L. Fiorillo, A. Bianchi, C. D'Amico, G. Amoroso, F. Gorassini, R. Mastroloni, S. Marino, C. Scoglio, F. Catalano, P. Campagna, S. Bocchieri, R. De Stefano, T.M. Fiorillo, M. Cicciò, Herpes virus, oral clinical signs and QoL: systematic review of recent data, *Viruses* 11 (5) (2019) 463, doi:10.3390/v11050463.
- [11] X. Dai, H.Z. Zhou, Structure of the Herpes Simplex Virus 1 capsid with associated tegument protein complexes, *Science* (6) (2018) 360, doi:10.1126/science.1257298.
- [12] D.M. Knipe, R. Whitley, *Encyclopedia of Virology: Herpes Simplex Virus 1 and 2*. Fourth Edition, Academic Press, 2021, doi:10.1016/B978-0-12-809623-3.821273-3.
- [13] M.G. Gopal, Kumar B C S Shannoma, R. M. S.N. A, N.C. Manjunath, A comparative study to evaluate the efficacy and safety of acyclovir and famciclovir in the management of herpes zoster, *J. Clin. Diagn. Res.* 7 (12) (2013) 2904–2907 Dec/Epub 2013 Nov 18. PMID: 24551671; PMCID: PMC3919380, doi:10.7860/JCDR/2013/7884.3670.
- [14] G.J. Greener, M.S. Kandathil, T.J. Jones, Deep learning extends de novo protein modelling coverage of genomes using iteratively predicted structural constraints, *Nat. Commun.* 10 (2019) 3977, doi:10.1038/s41467-019-13994-0.
- [15] H. Hassan, A. Khadija, A. Fauziah, F. Shamsuddin, R. Basir, Antiviral nanodelivery systems: current trends in acyclovir administration, *Hindawi* (2016) 4591634 Article ID, doi:10.1155/2016/4591634.
- [16] C. Jiang, H. Feng, C. Lin, X. Guo, New strategies against drug resistance to herpes simplex virus, *Int. J. Oral Sci.* 8 (1) (2016) 1–6, doi:10.1018/jios.2016.3.
- [17] C. Johnston, A. Wald, *Infectious Diseases, Genital Herpes*; Antiviral therapy, 4th Edition, Elsevier, 2017, doi:10.1016/C2013-1-00044-3.
- [18] N.M. Landis, *Topical and Intralesional Antiviral Agents: A Comprehensive Dermatologic Drug Therapy*, 4th Edition, Elsevier, 2021, pp. 493–503. PageSBN 9780323612111, doi:10.1016/B978-0-323-61211-1.100043-7.
- [19] K.J. Looker, A.S. Magaret, M.T. May, K.M. Turner, P. Vickerman, S.L. Gottlieb, Global and regional estimates of prevalent and incident herpes simplex virus type 1 infections in 2012, *PLoS ONE* 10 (10) (2015) 1371.
- [20] K.J. Looker, N.J. Welton, K.M. Sabin, S. Dalal, P. Vickerman, K.M.E. Turner, M.C. Boily, S.L. Gottlieb, Global and regional estimates of the contribution of herpes simplex virus type 2 infection to HIV incidence: a population attributable fraction analysis using published epidemiological data, *Lancet Infect. Dis.* (2020), doi:10.1016/S1473-3099(19)30470-0.
- [21] B.A. Nair, A. Mahesh, E.A. Bandar, W. Jyoti, H. Shree, A. Mueen, Enhanced oral bioavailability of acyclovir by inclusion of complex using hydroxypropyl- β -cyclodextrin, *Drug Deliv.* (2013) 540–547 Page, doi:10.3109/10777544.2013.853211.
- [22] K.K. Neelabhi, A. Jewara, K.S. Kumari, In-silico designing of NKK: a better ligand than aciclovir against herpes simplex virus, *Indian J. Pharm. Biol. Res.* 3 (1) (2015) 48–55.
- [23] M.N. O'Boyle, M. Banck, A.C. James, C. Morley, T. Vandermeersch, R.H. Hutchison, Open babel: an open chemical toolbox, *J. Cheminform.* 3 (2011) 33, doi:10.1186/1758-2946-3-33.
- [24] S. Oldham, B. Pöschel, L. Parkes, A. Amalkeviciute, C. Sun, A. Fornito, Consistency and differences between centrality measures across distinct classes of networks, *PLoS ONE* 14 (7) (2019) e0220061, doi:10.1371/journal.pone.0220061.
- [25] E.F. Pettersen, T.D. Goddard, C.C. Huang, G.S. Chu, D.M. Greenblatt, E.C. Meng, T.E. Ferrin, UCSF Chimera—a visualization system for exploratory research and analysis, *J. Comput. Chem.* 25 (13) (2004) 1605–1612.
- [26] M. Pinder, A. Wright, Valaciclovir versus aciclovir for the treatment of primary genital herpes simplex: a cost analysis, *Int. J. STD AIDS* 26 (13) (2014) 971–973. VolumeIssuePages, doi:10.1177/0956462414563628.
- [27] A. Reyes, A.M. Farías, N. Corrales, E. Tognarelli, A.P. González, Herpes Simplex Viruses Type 1 and Type 2 Infection and Immunity, Reference Module in Biomedical Sciences, Elsevier, 2021, doi:10.1016/B978-0-12-838711-9.00062-8.
- [28] A.J. Sadowski, R. Upadhyay, W.Z. Greesay, J.B. Margulies, Current drugs to treat infections with herpes simplex viruses-1 and -2, *Viruses* 13 (2021) 1228, doi:10.3390/v13071228.
- [29] P. Shamon, A. Markiel, O. Ozler, N.S. Baliga, J.T. Wang, D. Ramage, N. Amin, B. Schwikowski, T. Ideker, Cytoscape: a software environment for integrated models of biomolecular interaction networks, *Genome Res.* 13 (11) (2003) 2498–2504.
- [30] Shapovalov M.S. and Dunbrack R.L. Jr (2011) A smoothed Backbone Dependent Rotamer library derived from Adaptive Kernel Density Estimates and Regressions *Structure* 19, 844–858.
- [31] Steven McGee, *Evidence-Based Physical Diagnosis: Reliability of Physical Findings*, 3rd Edition, 2012, pp. 29–39. Pages, doi:10.1016/B978-1-4377-2207-5.00004-5.
- [32] G. Su, H.J. Morris, B. Demchak, D.G. Bader, Biological network exploration with Cytoscape 3, *Curr. Proteom. Bioinform.* 47 (8.131–8.13) (2015) 24, doi:10.1002/0471250953.b0813347.
- [33] Terry P. Kenakin, *Pharmacology in Drug Discovery and Development: Understanding Drug Response*, 2nd Edition, Elsevier, 2017, doi:10.1016/C2015-0-00443-9.

- [34] The PyMOL Molecular Graphics System, Version 2.3 r3pre, Schrödinger, LLC.
- [35] O. Trott, A.J. Olson, AutoDock Vina: improving the speed and accuracy of docking with a new scoring function, efficient optimization and multithreading, *J. Comput. Chem.* 31 (2) (2010) 455–461.
- [36] A.W. Watson, J.N. Rhodes, A.J. Echenique, P.M. Angarone, H.M. Scheetz, Resolution of acyclovir associated neurotoxicity with the aid of improved estimates using Bayesian approaches: a case report and review of literature, *J. Clin. Pharm. Therapeut.* 42 (3) (2017) 350–355.
- [37] J. Wang, W. Wang, F.A. Kollman, D.A. Case, Automatic atom type and bond type perception in molecular mechanical calculations, *J. Graph. Model.* 25 (2) (2005) 247–260 Page.
- [38] J. Xu, Y. Zhang, How significant is a protein structure similarity with TM-score = 0.5? *Bioinformatics* 26 (7) (2010) 883–895 Volume, pages, doi:10.1093/bioinformatics/btq066.
- [39] H. Yang, C. Lou, L. Sun, J. Li, Y. Cai, Z. Wang, W. Li, G. Liu, Y. Tang, AdmetSAR 2.0: web-service for prediction and optimization of chemical ADMET properties, *Bioinformatics* 35 (6) (2019) 1067–1069 Volume:issue:5 March 2019Pages, doi:10.1093/bioinformatics/bty707.
- [40] J. Yang, I. Anishchenko, H. Park, Z. Peng, S. Ovchinnikov, D. Baker, Improved Protein Structure Prediction Using Predicted Interresidue Orientations, 117, *PNAS*, 2020, pp. 1496–1503.
- [41] E. Zinser, A. Krawczyk, P. Mühl-Zürbes, U. Aiföderhorst, C. Draßner, L. Stich, M. Zaja, S. Strobl, A. Steinkasserer, C. Heilingloh, A new promising candidate to overcome drug resistant herpes simplex virus infections, *Antiviral Res.* (149) (2018) 202–210 VolumePages, doi:10.1016/j.antiviral.2017.11.012.

Appendix II: Patent Certificate


The Industrial Property Act, 2001

CERTIFICATE

OF GRANT OF A PATENT

It is hereby certified that a patent with patent number KE 947 has been granted to: **JOMO KENYATTA UNIVERSITY OF AGRICULTURE AND TECHNOLOGY (JKUAT)** of P. O. BOX.62000-00200, NAIROBI, Kenya in respect of an invention disclosed in an application number **KE/P/2021/3801** having a date of filing of 17/02/2021 and being an invention titled **ACYCLOVIR DERIVATIVE FOR TREATMENT OF HERPES SIMPLEX VIRUS.**

Dated at Nairobi this 25th day of November, 2022.


.....
John Onyango
Ag. Managing Director

(19)



(11) Patent Number: KE 947

(45) Date of grant: 25/11/2022

(12) PATENT

(51) Int.Cl.2016.01: A 61K 31/52, A 61P 31/22, A 61P 31/12

(21) Application Number:
KE/P/2021/3801

(22) Filing Date:
17/02/2021

(73) Owner:

JOMO KENYATTA UNIVERSITY OF AGRICULTURE AND TECHNOLOGY (JKUAT) of P. O. BOX.62000-00200, NAIROBI, Kenya

(72) Inventors:

CLIVE MOGAKA NYARIBO, BIOCHEMISTRY DEPARTMENT, SCHOOL OF MEDICAL SCIENCES, P. O. BOX 180-40500 NYAMIRA, KENYA; FLORENCE ATIENO NG'ONG'A, BIOCHEMISTRY DEPARTMENT, SCHOOL OF MEDICAL SCIENCES, P. O. BOX 62000-00200 NAIROBI, KENYA and STEVEN NYANJOM GER, BIOCHEMISTRY DEPARTMENT, SCHOOL OF MEDICAL SCIENCES, P. O. BOX 62000-00200 NAIROBI, KENYA

(74) Agent/address for correspondence:

DIRECTORATE OF INTELLECTUAL PROPERTY MANAGEMENT AND UNIVERSITY -INDUSTRY LIAISON, (JKUAT), P. O. BOX 62000-00200 NAIROBI, KENYA

(54) Title:

ACYCLOVIR DERIVATIVE FOR TREATMENT OF HERPES SIMPLEX VIRUS

(57) Abstract:

The present invention discloses an optimized acyclovir derivative, 2-[(6-methyl-6,9-dihydro-3H-purin-9-yl) methoxy]ethan-1-ol for development of a therapeutic drug for treatment of herpes simplex virus type 1 (HSV -1) and herpes simplex virus type 2 (HSV -2) diseases. The derivative was modelled and optimized through a computer aided drug design (CADD) using ChemsKetch Software. Also described is a method of synthesizing the acyclovir derivative, starting with guanine using tetrahydrofuran as solvent, C-N bond formation using Tetra-n-butylammonium fluoride and Dimethylformamide, Dess-Martin Oxidation and use of sodium hydroxide to incorporate the hydroxyl group. Also described is a method of formulating anti-herpes simplex virus drug, comprising 2-[(6-methyl-6,9-dihydro-3H-purin-9-yl) methoxy]ethan-1-ol as the active pharmaceutical ingredient (API) prepared by direct compression and wet granulation techniques. The lead compound optimization involves, removal of amine and replacement of carbonyl with methyl group to generate optimized derivative with increased bioavailability

